Final Report: ME 450 Winter 22

Bucsek Research Group, University of Michigan
Section 5: K. Alex Shorter
Team 18: James Lorenz, Jacob Raman, Kevin Thakkar, Richard Wall
April 22, 2022

In-situ/Operando Experimental Investigation of Battery Performance

Abstract

To keep up with emerging battery technologies, it is crucial to study the real-time performance of solid-state cells with the highest precision. Our manipulation device enables a variety of cell samples to be investigated under 3D x-ray microscopy from multiple angles during its operation. The results obtained would help quantify different battery performance metrics and compare material selection for battery development. Improvements in energy density, cycle life, and recyclability among others can serve as significant milestones in the next generation of battery energy supply and storage technologies across many industries and applications.

Executive Summary

The Bucsek research group has laid out an experimental setup to investigate the performance metrics of different battery materials and technologies. Using an in-situ (in position) operando (in operation) approach, this process would help study the microscopic changes in battery chemistry in real time. Compared to the traditional ex-situ methods, the precision in imaging and quantifying material behavior using advanced x-ray microscopy would be a significant development in analyzing specific battery performance metrics.

Since the research and commercialization of new battery technologies are developing at a faster pace than ever, the Bucsek Research Group's experimental setup would be a valuable addition to the field of cell-development. By characterizing real-time material behavior in terms of grain orientation, interphase layer fluctuations, dendrite growth, and void formation among other metrics, the results can help researchers select materials and electrochemical components of cells that can improve battery performance. To name a few, this can be in the form of improved energy density, cycle life, thermal stability, recyclability, and safety.

Our device would be located in the approximate center of the experimental setup where a cell with maximum diameter of 1 mm would be placed along the vertical axis for the x-rays to diffract through and be imaged on the far-field detector. The cell sample would also be placed on a 360 degree rotational base that would help capture multiple angles of the sample during operation. For this reason, our design requires the use of x-ray transparent materials (up to 90%) and be sealed airtight in a glove-box. To charge and discharge the cell sample, our design also requires a provision for current collectors at both ends that would connect to an external voltage source. We were also required to design mechanisms that would apply a vertical mechanical load to the cell leading to a maximum displacement of 25 microns, and apply heat to a maximum of 60 degrees Celsius. The budget constraint for this project was $1000, with a planned contingency for additional parts following our final design.

Implementing feedback from stakeholders through the process from concept generation to the final design, we were able to iterate multiple options to deliver our best solution to the problem statement.

In our final design, we delivered an assembled prototype manufactured using 3D prints, CNC, and waterjetted parts well within our budget at $137. This final prototype was also analyzed, verified, and validated both theoretically and empirically to the best of our abilities within the timeline constraints. Apart from the cost-restrictive motorized loading system, all components in the final design successfully met the list of requirements and specifications. Our sponsor also provided us with positive validation for our design and looks forward to building on the prototype for implementation in the experimental setup.

Table of Contents

Project Introduction, Background, and Information Sources

As the global energy industry evolves to integrate renewable sources, energy storage, and more efficient power solutions, battery technologies are foundational to accelerate the transition across multiple industries. These include electric mobility vehicles (EVs), electronic devices, and storage systems among many others. Batteries and cells are at the core of powering these technologies, and also the overarching focus of the Bucseck Research Group for this project. As of 2022, the most widely used commercial solution is the lithium-ion battery which has a set of limitations that need to be overcome for the next generation of batteries. From the unsustainable mining of lithium metal, performance limitations, safety concerns, and recycling problems, the next material solutions should be able to address these challenges and be a commercially viable alternative.

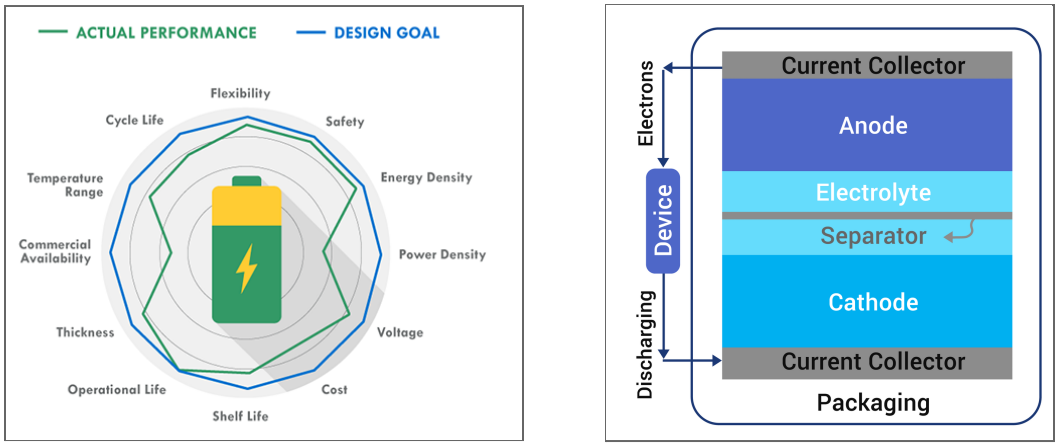

(a) **(b)**

Figure 1. Graphic (a) lists various battery performance metrics that are important for the technical performance and economic feasibility of battery solutions.[2] The green line represents a sample performance distribution for a current technology. The blue line represents the ideal solution to possibly achieve improved performance across all metrics. Diagram (b) shows the different electro-chemical parts of a solid state battery cell. The anode is the negative terminal of the cell, and the cathode is the positive terminal.[1] The cell is charged when the applied current causes electrons to transfer from the cathode (+) to anode (-) from the electrolyte. The interface between the anode and electrolyte is the specific focus of our sponsor's research in investigating the microscopic material changes that occur at and around this surface.

The goal of our sponsor's research is to create an experimental setup that would enable the investigation of different cell material samples and consequently push the distribution of these metrics represented in Figure 1(a) as close to the blue line as possible.

To meet this goal, the Bucseck Research Group has designed an experimental setup that uses advanced x-ray devices to study the microscopic changes in a cell from all angles during its operation. More specifically, the metrics being studied include the growth of the anode-electrolyte layer, void formation, grain orientation, and the impact of external heat and load. Conducting these experiments on different materials of cell samples would help study and compare the performance of these batteries as intended. This 'in-situ' method would provide more precise information about battery performance as compared to the traditional 'external' method that cannot capture real-time information at such a small scale.

Therefore, our problem statement was *"To design and fabricate a device that holds a cell sample within the x-ray microscope, supplies a current to the cell, and applies a mechanical and thermal load during operation."*

Since this manipulation device needs to be custom designed for the setup and a variety of cell samples and operating conditions, our goal was to design the device around the sponsor's requirements as listed in the sections ahead. A successful deliverable would meet these requirements and specifications with a manufactured prototype that is tested for verification and validation as well.

Given that the use of in-situ and operando analysis is a relatively new technology, literature reviews of other research groups and scientific journals provide limited design solutions for this particular device.This information was collected, evaluated, and referenced with the guidance of a librarian to refine our approach in defining the background and context of our design.

Using a robust design framework based on our timelines, we were able to develop and deliver a final design to our sponsor that will be placed within the experimental setup seen in Figure 2 below.

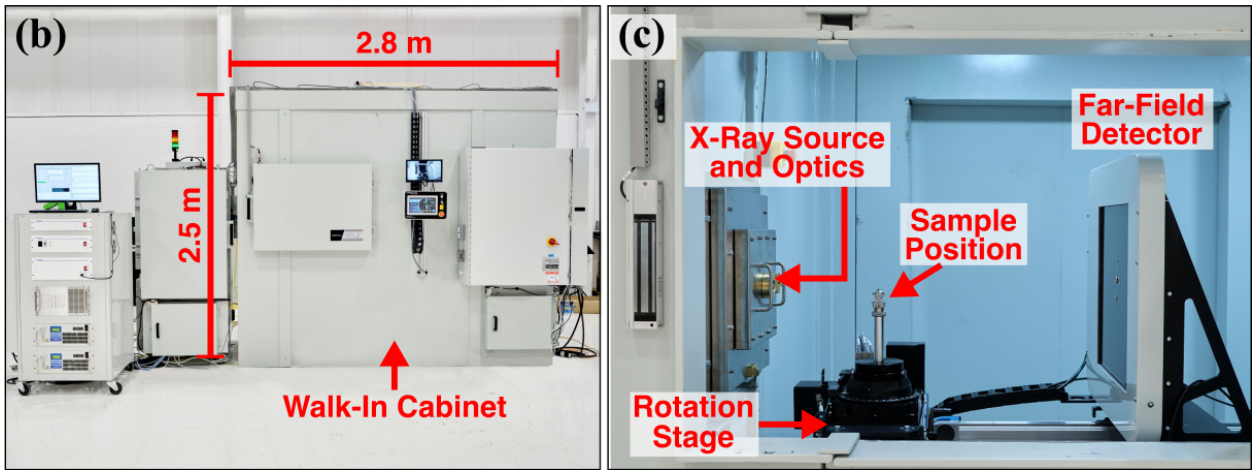

Figure 2. The experimental setup shows the full x-ray microscope on the left (b) and inside of the cabinet on the right (c)[12]. The inside of the cabinet shows the Bucsek group's current methodology for holding a cell sample; a metal rod with what is essentially a "vice" grip attached on top of the rotation and mounting stage.

Stakeholder Analysis

Since the application of our device is in laboratory setups, our primary stakeholders include researchers and groups that are interested in battery materials selection and high-accuracy performance analysis. Any researchers who want to conduct x-ray microscopy experiments in real time will benefit from the delivery of a design and prototype produced through this design project.

Secondary stakeholders of this project may include the beneficiaries of the research results. This list includes but is not limited to - battery manufacturers, corporations in the electronics business, and electrode metal mining companies. Many of these stakeholders will be affected positively by the final deliverables of this project. However, there may be some negative outcomes for these stakeholders. For example, mining companies engaged in lithium extraction may need to switch to mining different metals based on the future requirements of the industry.

Tertiary stakeholders include the end-users of the improved battery products. Customer applications can range from electric vehicles (EVs), to energy storage systems, electronic devices like mobile phones and computers, and many more as traditional energy systems are on the route to electrification. A layout of this stakeholder analysis is summarized in Figure 3 below.

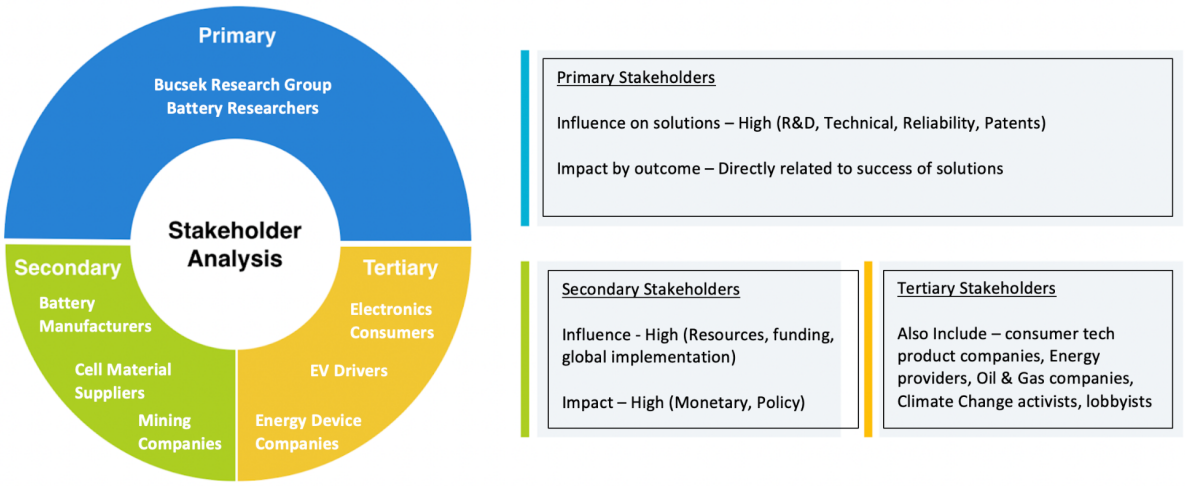

Figure 3. Stakeholder map and analysis for the Bucsek Group's research implications.

Design Context

In the coming decades, it is projected that cumulative demand for lithium ion batteries for electric vehicles and other energy storage applications will increase exponentially.[8] This demand, coupled with recent activism and attention to switch from fossil fuels to renewable energy sources, has significantly expanded research into more advanced electrical energy storage and battery technologies. More specifically, because lithium ion batteries are currently the "gold standard" for battery material selection and composition, research into improved battery material selections has seen greater focus.[4] Lithium ion batteries also present safety hazards in their current state. The rising demand for renewable energy alternatives, such as electric vehicles, coupled with the status quo of battery material options being dominated by lithium-ion batteries, means that engineers must strive for significant improvements in battery technology to increase public safety in regards to battery implementation.

A successful design and prototype delivered from this design project can add an additional testing element to a growing cohort of real-time battery testing. The more temporal data of battery material changes that researchers and engineers have access to will allow for the selection of materials that have better energy density, cycle life, and stability while also increasing safety for end users.

The device itself is estimated to have a minimal environmental impact. The decision was made early on, in coordination with the primary stakeholders, that the deliverable design and prototype device would be intended for more than one use. This decreases the environmental impact of the design from manufacturing parts, the purchase and delivery of materials, and of potential waste disposal. The use of the device in an x-ray microscopy lab experiment will have some environmental impact due to the power source necessary to run the sample battery cell, but this impact is miniscule. Sustainability is a major concern that engineers must grapple with when engaging in the design process. The multi-use nature of the final device prototype also minimizes the use of resources towards a sustainable design.

There are some elements of the project that can be unsustainable. Mainly, the procurement of battery cell samples for testing in the device, or any other analogous materials, is not a sustainable process. The battery cell samples require rare materials in order to fabricate or will need to be purchased in large quantities and shipped to the testing site. Additionally, the cell samples will degrade during experimentation in the device and will need to be disposed of which may not be done in a sustainable manner. We do not anticipate that any of our personal ethics will differ from the expected ethical considerations we are to uphold as students working at the University of Michigan

Design Process

Thus far in this semester we have followed the ME Capstone Design Process Framework because of the framework's comprehensive approach to the design process that can be scaled to large-scope projects. This particularly suits our project because we are designing an entire mechanical system with dynamics, heat transfer, and electrical subsystems, which requires a holistic approach to the design process. While we considered an activity-based model to suit the diverse tasks required for this project Wynn and Clarkson, we felt that a stage-based design was more suitable for this project to allow for multiple tasks to be addressed in parallel by different subteams. With the added flexibility that the ME Capstone Framework provides and emphasis on project-long learning/synthesis of relevant information in the field of solid-state batteries, we eventually settled on this framework as the best approach to address the sponsor's need for this project.

Following this framework, we also conducted a functional decomposition of our device during the concept generation phase. This helped us break down the requirements into a set of functional solutions, which were then evaluated based on our ranked design preferences and ease of implementation within our project timeline. Our design selection process is described in further detail in following sections.

The framework for the design process throughout the project is shown in Figure 4 below.

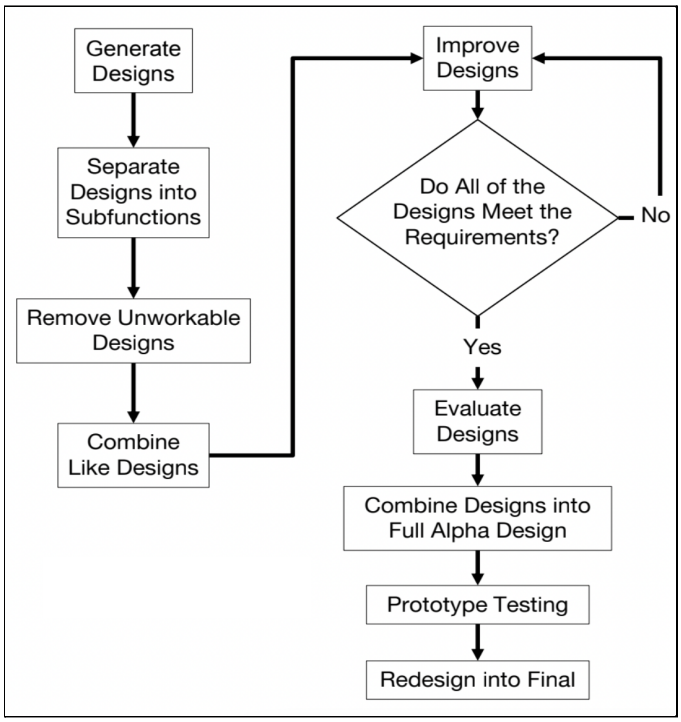

Figure 4. Design process flow diagram employed from our concept generation to final prototype.

Requirements and Engineering Specifications

To start determining the requirements, we approached it beginning from the minimum elements necessary for a functional device. This includes the ability to hold the sample and allow the sample to be observed by the x-ray microscope all while ensuring the sample does not come in contact with oxygen gas.[12] The device also needs to operate the sample by providing a voltage across it.[12] The sponsor also said that to get satisfactory measurements, they need the ability to rotate the sample while it's being measured. These are the minimum requirements necessary for the device to work. Other requirements the sponsor would like would be the ability to apply heat and a mechanical load, though these are not completely necessary.[12] There are also basic requirements of keeping the cost low and making it easy to assemble and transport, but they may be dropped to satisfy other requirements if needed. A full list of the requirements along with their corresponding specifications and sub-functions can be found in Table 1.

Table 1. List of requirements ordered by decreasing importance with the corresponding specifications

Requirement		Specification
Hold	Must be able to hold the sample	Fixture must be able to hold a sample with a diameter of 1 mm and height between 0.1-2 mm^2
	Sample must not touch oxygen	Sample must be held in a sealed container at 1 atm with airtightness of 2 $cc/cm^2/24hr$
Observe	Allow the sample to be observed by x-ray microscopy	Non-battery materials in the incident and diffracted beams of the x-rays should be at least 90% x-ray transparent at 18 keV. Incident beam - 1.5 x 0.5 mm Diffracted beam - 40 degree cone
	Sample must be measurable from multiple angles	Fixture should be able to handle rotation so that the battery sample can be observed 360 degrees around the vertical axis
Run	Supply voltage to the sample	Must be able to connect to a power supply and provide 1 to 4 volts to the sample
Load	Apply a mechanical load to the sample	Apply and measure a load along the vertical axis to the battery sample of up to 25 micron displacement with accuracy of 0.1 microns
Heat	Apply heat to the sample	Apply heat of up to 60°C to the sample during operation
Misc.	Low cost	Must cost less than $1000 per measurement
	Easy to assemble	Fixture must be able to be assembled with at most 2 tools
	Easy to transport	Fixture must weigh less than 35 lbs

Concept Generation

The team first split up to generate concepts individually using divergent thinking, examples of which are shown in appendix A, Figure A1. All types of designs were considered, even those that would not match the requirements. Once each team member generated sufficient designs, the team met up and, using convergent thinking, eliminated designs that were obviously infeasible and could not work with the requirements listed above. The remaining designs were decomposed into each of their various sub-function: holding the sample, observing the sample, running the sample, (mechanically) loading the sample, and heating the sample. Quickly, the "Hold" sub-function was combined with the "Run" sub-function as all feasible designs generated used the electrical leads to support the sample. Similar designs were then combined, leaving a set of ten designs across the sub-functions which were then refined via an iterative process. Refined designs for each sub-function are shown in Figure 5. The rest are shown in appendix A, Figures A2-A5.

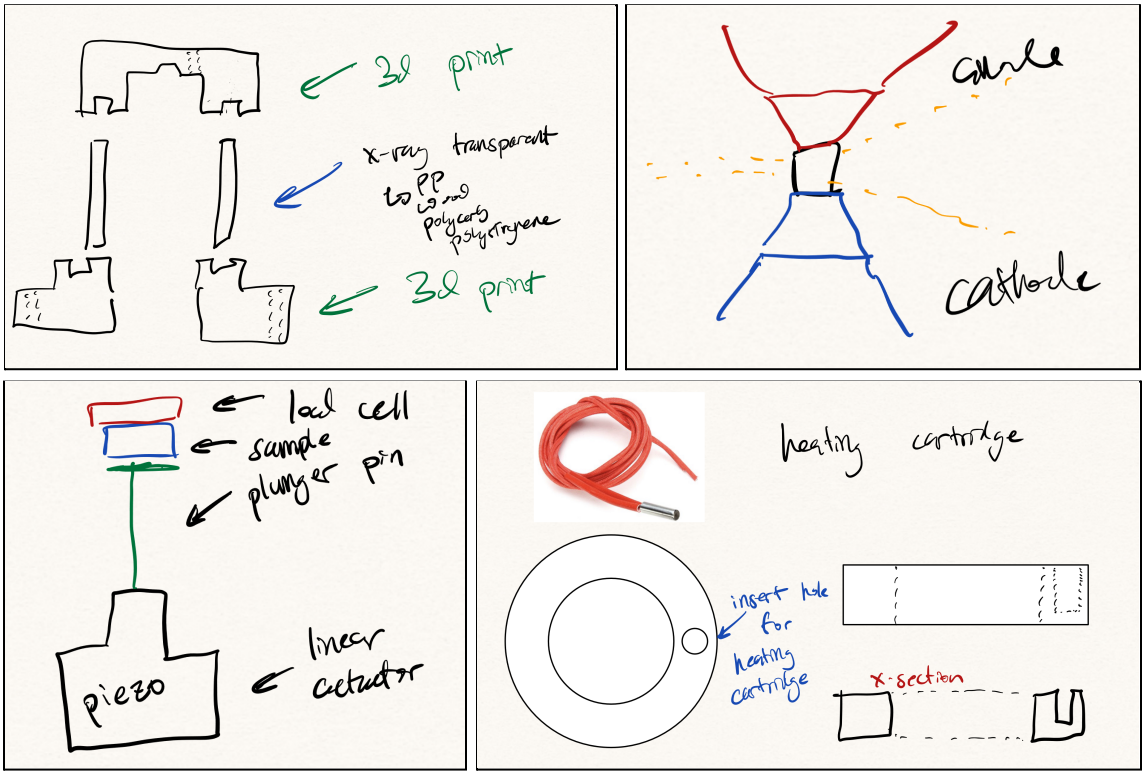

Figure 5. The top left design is for observing the sample. The top right design is for running and holding the sample. The bottom right design is for loading the sample. The bottom left design is for heating the sample.

The designs for observing the sample focus on allowing x-rays to pass through from any. The design in Figure 5 attempts to accomplish this by having a thin cylindrical window of x-ray transparent material to surround the sample, this does make the container more difficult to assemble than other designs as each interface between parts needs to be sealed to stop air from reaching the sample.

The designs for running the sample were combined with the designs for holding the sample and focus on supporting the sample while ensuring that the electrical leads connect to the sample and do not interfere with the x-ray beam. The design in Figure 5 attempts to accomplish this by providing a narrow platform for the sample to sit while expanding out away from the sample to create a larger, more stable base. The

narrow contact, while providing stability, still runs the risk of the sample falling off if it gets bumped and, depending on the size of the beam, might still interfere with the measurements.

The designs for loading the sample focus on providing a precise and accurate load that can be easily measured. The design in Figure 5 attempts to accomplish this by using a high-precision linear actuator to press the sample against a load cell which would then measure the resulting force. Given that the linear actuator is purchased off-the-shelf, it is easy to ensure it meets the required precision and accuracy, however such an actuator is going to be quite expensive and possibly over budget.

The designs for heating the sample focus on providing an accurate and consistent temperature to the sample. The design in Figure 5 attempts to accomplish this by using a heating cartridge to heat up a metal ring which would then heat up the argon inside the container and thus heat the sample. There would most likely be a thermistor somewhere inside the container to measure the temperature. While the consistency isn't much of an issue as one can simply wait for the temperature to reach steady-state, the method is not very precise given that it relies on indirect heating.

Concept Selection Process

Once the different designs were generated, an evaluation matrix was created for each sub-function. The designs were then ranked and the best one chosen. The evaluation matrix for holding the sample is shown in Table 2 and the other matrices are in appendix A as Tables A1-A3.

Table 2. Evaluation matrix for the "Observe" sub-function. Design 1 refers to the design shown on the left side of Figure A2 in appendix A. Design 2 refers to the design shown in the top left of Figure 5. Design 3 refers to the design shown on the right side of Figure A2. Both design 1 and design 2 had the same weighted total, however the team selected design 2 given that it scored better in x-ray transparency, the highest weighted category.

Criteria	Design 1	**Design 2**	Design 3
Ease of manufacturing (0.1)	4	2	2
Ease of assembly (0.3)	4	4	2
Structural strength (0.2)	5	2	3
x-ray transparency (0.4)	2	4	4
Weighted Total	3.4	3.4	3
Rank	2	**1**	3

The concept chosen for observing the sample was the one shown in the top left of Figure 5, which used a transparent window to allow for the x-ray to pass through. This design scored well for x-ray transparency, which was deemed by the team to be the most important category. It is, however, more difficult to manufacture and not as strong structurally as the others.

The concept chosen for running/holding the sample was the one shown in the top right of Figure 5, which used a narrow contact to support the sample while trying to avoid the x-rays. The evaluation matrix for this is in the appendix as Table A1. This design is not the best at supporting the sample or avoiding the x-rays, however it tries to get a good balance between the two.

The concept chosen for loading the sample was the one shown in the bottom left of Figure 5, which used an expensive linear actuator to achieve the precision and accuracy required. The evaluation matrix for this is in the appendix as Table A2. This design fits all of our requirements except for going over on cost, though it should be noted that all of the designs are fairly expensive given the necessity of a highly accurate load cell. While a requirement, keeping the device low cost was not a strict one. As such, the benefits of the high-precision linear actuator were deemed worth the added expense.

The concept chosen for heating the sample was the one shown in the bottom right of Figure 5, which used a heating cartridge to heat a metal ring that would heat the argon inside the container. The evaluation matrix for this is in the appendix as Table A3. The two designs were quite close, however this design was deemed to be the best as it provides, with the thermistor, a more accurate reading of the temperature of the sample. There is an issue however, of having to wait for the interior to reach steady-state conditions.

Design Concept Description

Following the concept generation process, the final designs selected for each of the four functional requirements were merged together in a single system to produce the design concept for the x-ray microscopy device prototype. Starting with hand-drawn concepts as shown in Figure A6 in appendix A, the design of these subsystems under a single system was critical not only to produce a single prototype, but also to confirm that the selected concepts from the functional decomposition process were not incompatible when integrated into a single package. Considerations for the small scale of the cell sample, volumetric constraints within the x-ray microscope, and radiolucency requirements of this mechatronics project were accounted for when designing the packaging for the four functional concepts. Once an integration design of these subsystems was drawn out, a virtual model of the design was built using computer-aided design (CAD) software. A CAD model of the design concept is shown below in Figure 6.

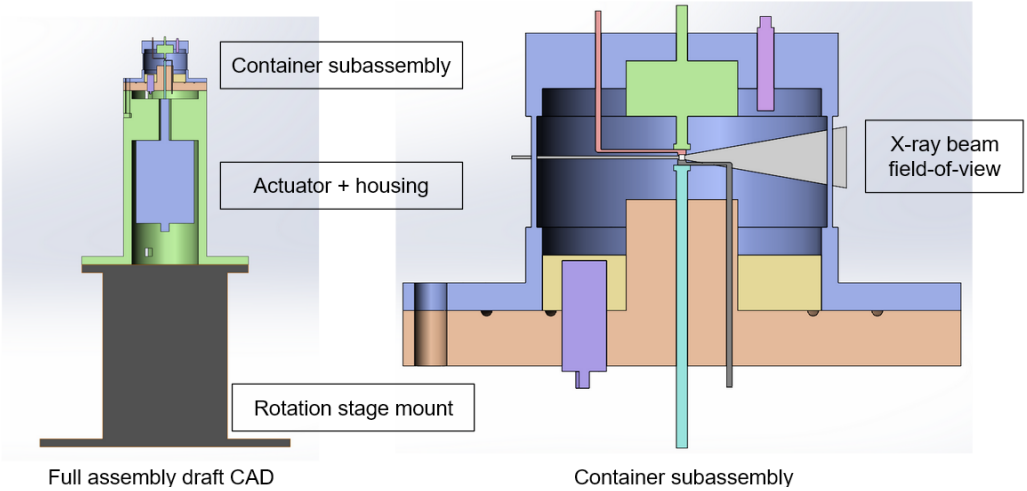

Figure 6. A cross-sectional overview CAD design is shown on the left. On the right are the container sub-assembly and actuator housing sub-assembly with the linear actuator, housing, and mounting hardware to the rotation stage on the x-ray microscope. The view on the right also shows the x-ray beam penetrating into the left side of the container, through the sample, and diffracting out from the right end.

Sample containment subsystem. The sample containment subsystem forms the outer shell which houses the cell sample. Its main function is to hold the cell sample precisely in the path of the x-ray beam during operation in a hermetically sealed inert atmosphere, without impeding the ingress or egress of the x-ray beam. The primary components of this subsystem are highlighted below in Figure 7.

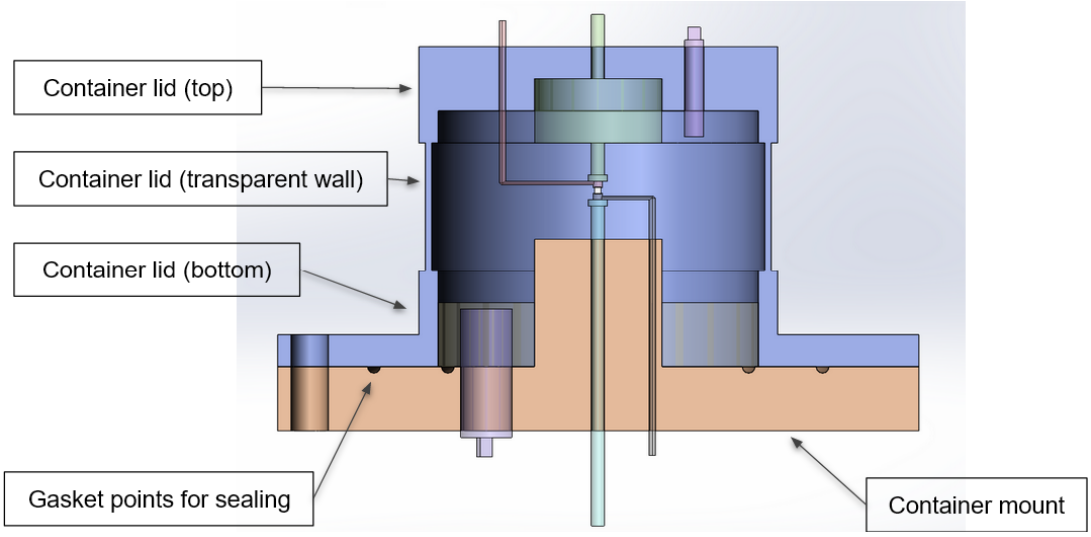

Figure 7. Sample containment subsystem CAD model, in a cross-sectional view. The container lid - consisting of three separate components - is shown in purple. The container mount is shown in orange. This subsystem, once the heating and electrical subsystems are mounted in place, is assembled in an inert atmosphere glove box.

Electrical application subsystem. The electrical application subsystem contacts the upper and lower surfaces of the cell sample to provide electricity to the cell. Its main function is to simulate an operating battery cell during testing by running a current through the sample. The primary components of this subsystem are highlighted below in Figure 8.

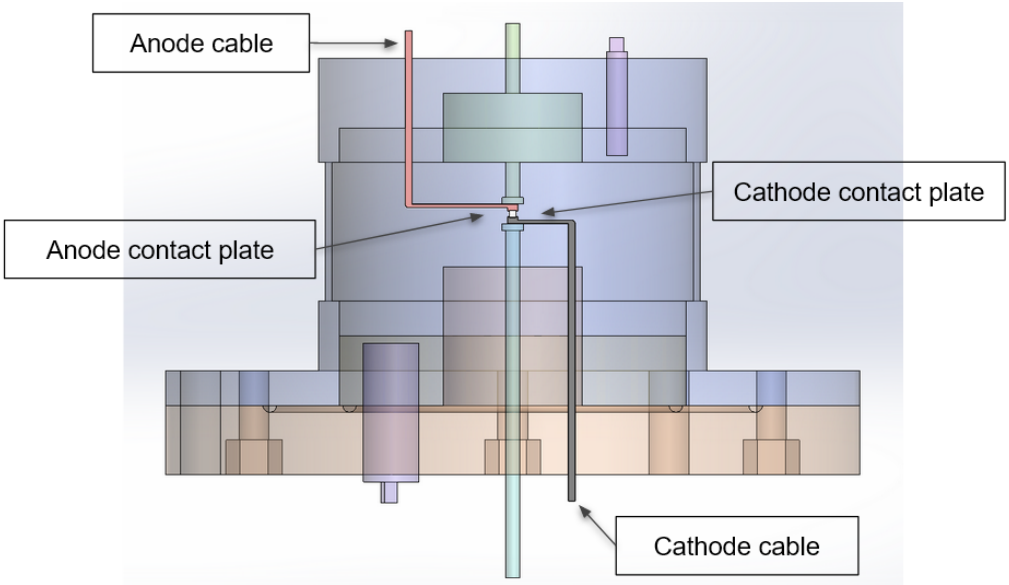

Figure 8. Electrical application subsystem CAD model, in a cross-sectional view. Anode cable from the top of the container subassembly soldered to the anode contact plate, shown in red. Cathode cable from the bottom of the container subassembly soldered to the cathode contact plate, shown in black. Electrical current flows through the call sample from the anode plate to the cathode plate.

Heat application subsystem. The heat application subsystem interfaces with the sample containment subsystem to evenly heat the interior of the container. Its main function is to provide a heated atmosphere for the cell sample to test the sample's performance under different steady state temperatures. The primary components of this subsystem are highlighted below in Figure 9.

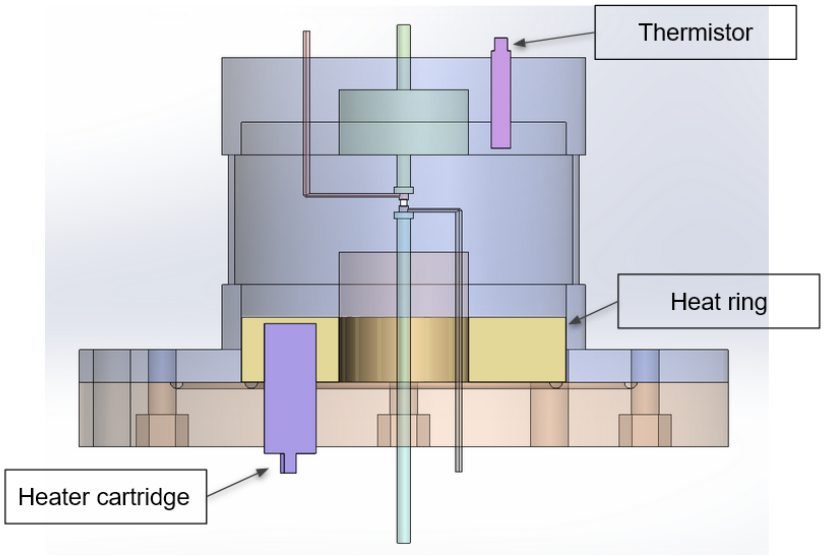

Figure 9. Heat application subsystem CAD model, in a cross-sectional view. Heater cartridge from the bottom of the container subassembly heats the heat ring. Heat ring heats the air inside the container subassembly, which in turn heats the cell sample. Internal air temperature is measured via a thermistor mounted on the top of the container subassembly, opposite the heater cartridge.

Stress application subsystem. The stress application subsystem applies a force to the upper and lower surfaces of the cell sample. Its main function is to provide an axial compressive stress to the cell sample to test the sample's performance under different loading conditions. The primary components of this subsystem are highlighted below in Figure 10.

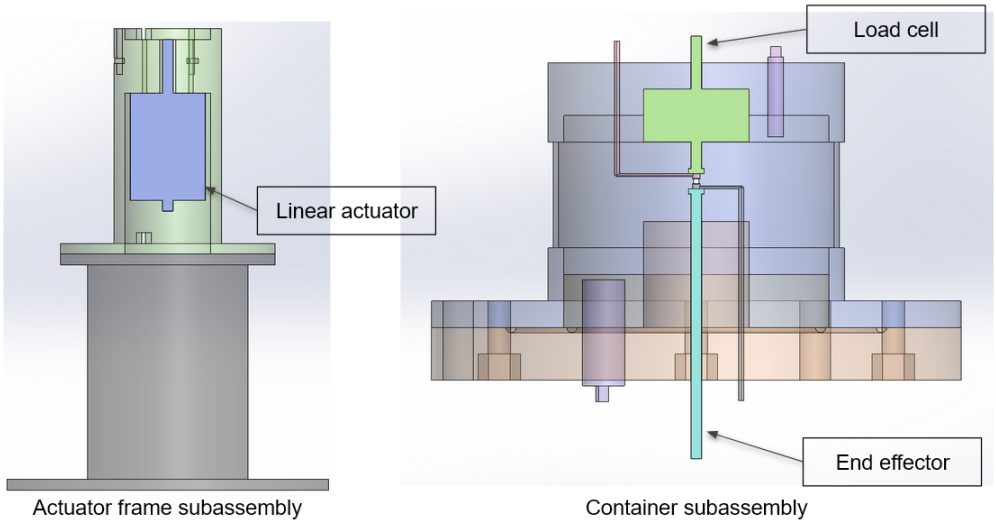

Figure 10. Stress application subsystem CAD model, in a cross-sectional view. The linear actuator is mounted within the actuator frame subassembly. The end effector, attached to the linear actuator, extends into the container subassembly, interfacing with the cathode contact plate. Force is applied by the linear actuator, through the end effector and contact plate, to apply a stress to the sample cell. Force is transferred through the cell and anode contact plate, to be measured by the load cell.

Engineering Analysis

To further improve upon the selected concept and alpha design, a combination of theoretical analysis and simulations were conducted. The goal of these analyses was to optimize and further refine the alpha design's sub-systems to affirm each selected concept's ability to meet the sponsor requirements and engineering specifications. Analysis was performed iteratively through the previously utilized functional decomposition: holding the sample, observing the sample, running the sample, [mechanically] loading the sample, and heating the sample. The primary purpose for performing these analyses was to further evaluate the selected design with respect to the requirements and specifications and make any necessary improvements to the design before proceeding with purchasing of materials, manufacturing, assembly, and verification testing.

Sample holding analysis. The sample holding analysis qualifies the subsystem's ability to hold the cell sample in place during x-ray operation and to provide an airtight, inert environment for the sample.

The alpha CAD model was thoroughly inspected to prevent any allowance of loose play in the system to determine the container's holding performance.

Drawing on the field of solid mechanics, a simple free body diagram of the cell sample was constructed to determine if adequate static friction is applied to the sample; this is shown in Figure 11.

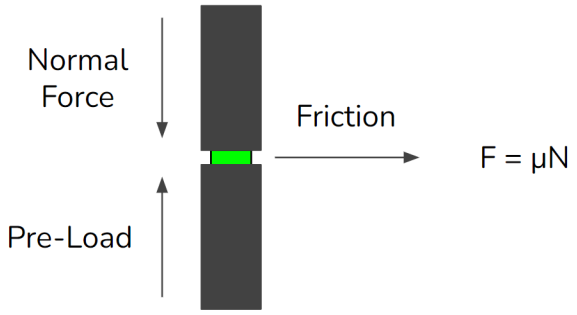

Figure 11. The simplified free body diagram of the holding rods shown in gray and the battery cell sample shown in green. Vertical normal force and preload force exerted in opposite directions on the sample while horizontal static friction forces act on the sample and help to keep it in place.

There are two vertical forces that will act on the cell sample, a normal force and a preload force. This preload force will be applied to the sample by the holding rod on the bottom of the sample; the alpha design shows how the end effector can be physically manipulated, either by pushing or screwing, to apply the force to the holding rod and thus to the sample.

Due to the time constraints of this academic term, no simple motion simulation was done using dynamics software to verify the stability of the sample. This is a potential avenue for further investigation, however it may not be necessary. Stability of the sample should be ensured by a manufactured "divot" in the holding rods. Additionally, the pre-load force theoretically provides an adequate hold on the sample.

The airtightness of the alpha design was not computationally analyzed. The design, and its further iterations, attempted to reduce the number of openings to the sample container. Any of the remaining openings were designed specifically as entry points for wires, linear actuator pistons, and out of necessity for assembly. These entry points will be sealed through various methods including silicone sealant, O-rings, and grommets. The reliability of these sealing methods is entrusted to the manufacturers and vendors these items will be purchased from.

Sample observation analysis. In the alpha design concept that was selected, there are materials that are required to be x-ray transparent so as not to interfere with the beam or diffraction patterns that will image the sample. Materials that are not x-ray transmissible will prevent diffraction patterns from reaching the far-field detector of the x-ray microscope experiment. These diffraction patterns are crucial for imaging the sample and capturing the internal material changes that are being investigated.

The alpha design planned for a thin 360-degree transparent window around the housing container of the sample. Metal contact plates were included in this design iteration as the current supply for eventual battery cell samples. In the final design, it is required that any materials that come in contact with the incident x-ray beam, and diffracted x-rays, must be at least 90% x-ray transmissible [transparent].

To analyze material selection choices for both the transparent window and the sample current supply, an open source x-ray transmission calculator was utilized. The Berkeley Lab Center for x-ray Optics (CXRO) has a publicly available x-ray transmission of solids calculator[22] that allows users to inspect a material's x-ray transmissibility. The necessary inputs are the chemical formula for the material, the density of the material in gm/cm^3, and the thickness of the material in microns. Additionally, a photon energy range of the x-rays in eV must be specified along with a step size less than 500 eV.

Many metal materials, like the copper alloy contact plates planned for in the alpha design, were discovered to have very poor x-ray transmissibility. Figure 12 illustrates the poor x-ray transmission of the copper alloy of density 9.4 gm/cm^3 and a thickness of 2000 microns. Due to this result, new materials would need to be investigated for holding and running the sample that would meet the threshold of at least 90% x-ray transmissibility.

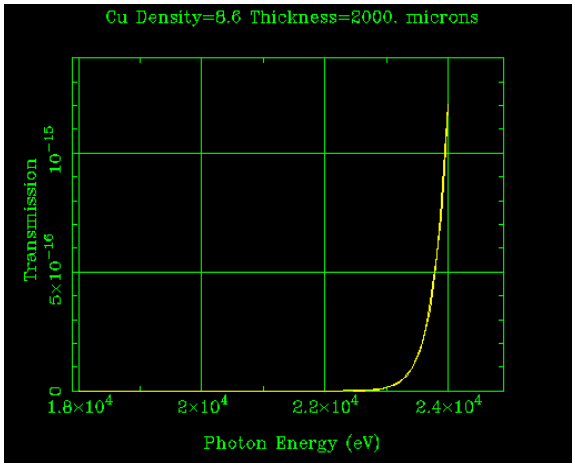

Figure 12: This graph displays the calculated x-ray transmissibility of pure copper. The photon energy range was selected to be between 18 keV and 24 keV per the Bucsek Research Group's operating procedure with their x-ray microscope. The copper configurations calculated here result in extremely poor x-ray transparency across the x-ray photon energy range.

One constraining factor in finding a substitute for copper was that the eventual selection had to be electrically conductive. The copper plates from the alpha design were included because they would connect the electrical current flow to the sample. Electrically conductive graphite rods became the focus of the analysis. The graphite inputs to the CRXO solid material x-ray transmission calculator were a chemical composition of C, a density of 1.3 gm/cm^3, and a thickness of 1588 microns. The results displayed in Figure 13(b) show that the graphite will provide adequate x-ray transmissibility, having an x-ray transmission rate of just over 90% within the specified x-ray energy range.

The (a) and (b) components of the transmissibility test are shown in Figure 13 below.

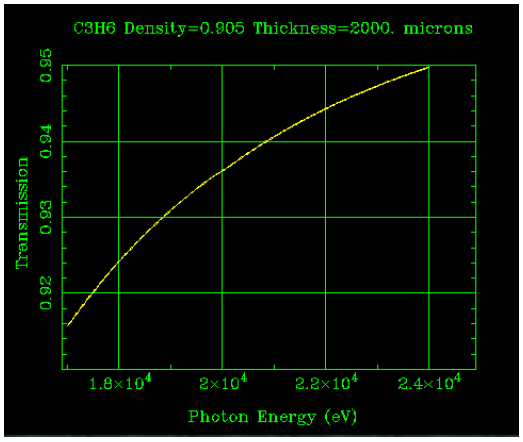

(a)

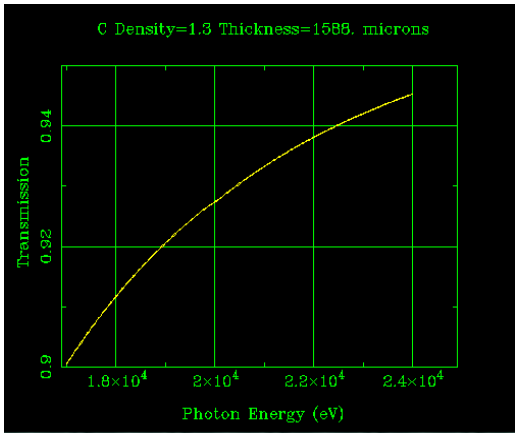

(b)

Figure 13: These graphs display the calculated x-ray transmissibility of polypropylene (a) and graphite (b). The photon energy range was selected to be between 18 keV and 24 keV per the Bucsek Research Group's operating procedure with their x-ray microscope. Both the polypropylene and graphite configurations calculated here result in above 90% x-ray transparency at at least 18 keV.

Polypropylene was an initial choice of material for the thin transparent window that would surround the sample. The polypropylene inputs to the CRXO solid material x-ray transmission calculator were a chemical composition of C_3H_6, a density of 0.905 gm/cm^3, and a thickness of 2000 microns. The results, displayed in Figure 13(a) indicate that the polypropylene has excellent x-ray transmissibility, having an x-ray transmission rate of over 92% within the desired x-ray energy range.

Electrically running the sample analysis. No major analysis was done to evaluate the design and its ability to run the battery cell sample. The alpha design included commercial wires that would connect to copper plates which would in turn complete an electrical current flow with the cell sample. These copper plates were eliminated from the design after the previous iteration of analysis showed they would be unconducive for x-ray beam and diffraction pattern transmission. The updated design iteration includes graphite rods that are electrically conductive. In future work, the surface resistivity of graphite and other materials would be of some interest. The relationship between electrical resistance and geometry is worth investigating in detail and analysis in this area could improve the current delivery mechanism.

Heating analysis. Engineering analysis for the heating subsystem was an additional scope of this project. In continuing this project, it may be useful to perform analysis and quantify the subsystem's ability to heat the cell sample to a steady state temperature. We recommend a simple heat transfer simulation conducted using a finite element analysis (FEA) software package. This simulation model can inform any design changes of this subsystem's components, and can be empirically verified by future manufactured heat sources. This simulation can also inform the design of a feedback loop using a thermistor.

Mechanical load application analysis. Analysis for mechanically loading the sample was not performed because this subsystem was not going to be incorporated into the final prototype this semester. This was due to both time constraints and also the monetary cost of procuring a piezo-electric linear actuator. However, future mechanical load and stress application analysis will quantify the subsystem's ability to deliver a steady and even load to the sample. We propose that a free body diagram be constructed in conjunction with a stress-strain model of the end effector and cell sample to theoretically verify the axial compressive stress induced to the sample. Another supporting analysis to conduct would be a calculation of the stress induced to a sample from the distance moved by an end effector; this relationship is key to understanding the minute amount of stress that needs to be applied to the sample.

Final Design Description

A final design using the analysis described above was made as a virtual model featuring the decided upon materials and parts. The final design does not differ significantly from earlier iterations explored during the design concept phase, apart from the electrical application subsystem and frame sub-assembly. The full design is shown in Figure 14 below.

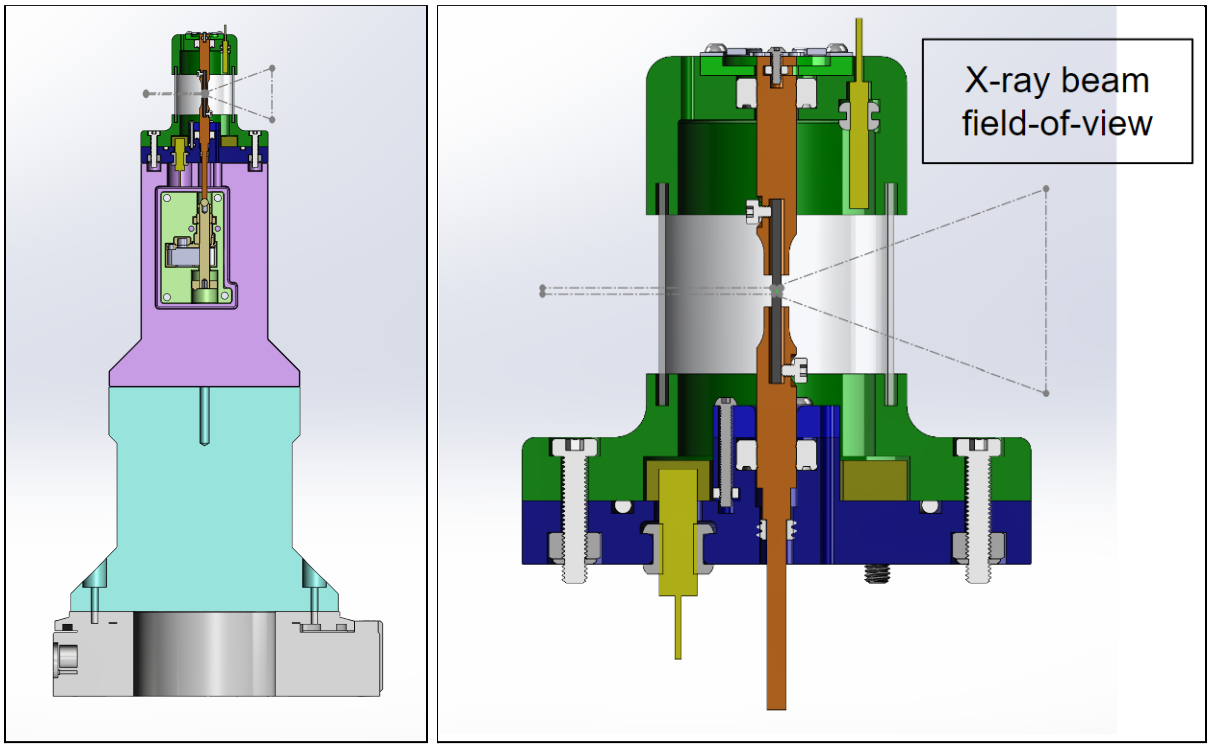

Figure 14. The final design. The sample container and frame (left) are attached to the mounting stage in gray on the bottom. The sample container (right) is shown with the field-of-view of the x-ray beam.

The main assembly of the final design consists of two subassemblies: the container subassembly and the actuator housing subassembly. The container subassembly houses the sample containment subsystem, the electrical application subsystem, and the heat application subsystem. The actuator housing subassembly contains the stress application subsystem and interface components for mounting the device to the x-ray microscope.

A physical version of this final design was manufactured and assembled for the purposes of verification and validation of the design concept. Furthermore, if the physical prototype is found to fulfill the functional requirements related to containing and running the sample, the device will be left in the possession of the sponsor for use as a laboratory instrument. Images of the fully assembled physical prototype, as well as an isometric view of the corresponding CAD model, can be seen in Figure 15 below.

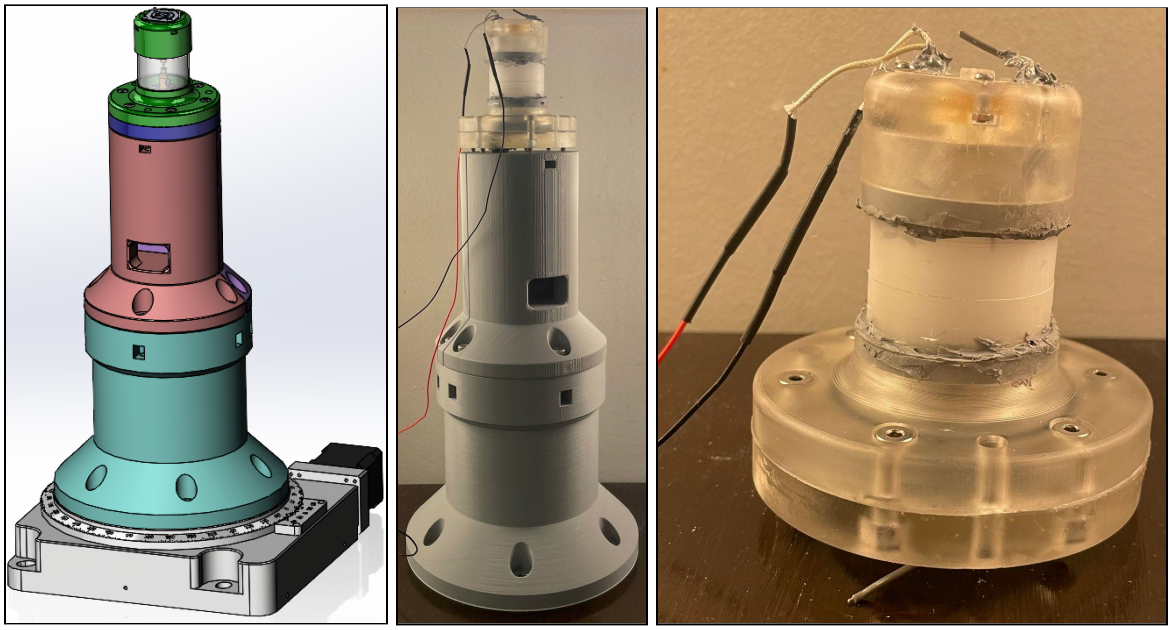

Figure 15. Physical prototype of the final x-ray microscopy device design compared to CAD model of final design. This build model was manufactured with the processes detailed in the Manufacturing Plan and assembled using the parts and materials found in the Bill of Materials. Structural components were 3D printed via SLA and FDM processes. The heat ring, transparent window, and graphite rods were CNC milled. Fasteners and sealing components were purchased commercially. Purchases of the load cell and linear actuator were omitted for the purposes of this report. Assembly was conducted manufally by two individuals, with no jigs or holding devices required for construction. All empirical validation tests were conducted using one or more of the subassemblies built for the physical prototype.

For each of these subsystems, detailed descriptions of material selections, off-the-shelf parts descriptions, and manufacturing plans can be found in the Bill of Materials and Manufacturing Plan sections found at the end of this report.

Sample containment subsystem. The sample container features the same basic design as in earlier revisions with the individual materials chosen after analysis. Notably, the window has been separated from the lid and is now made of 1mm thick polypropylene. The subsystem is shown in Figure 16.

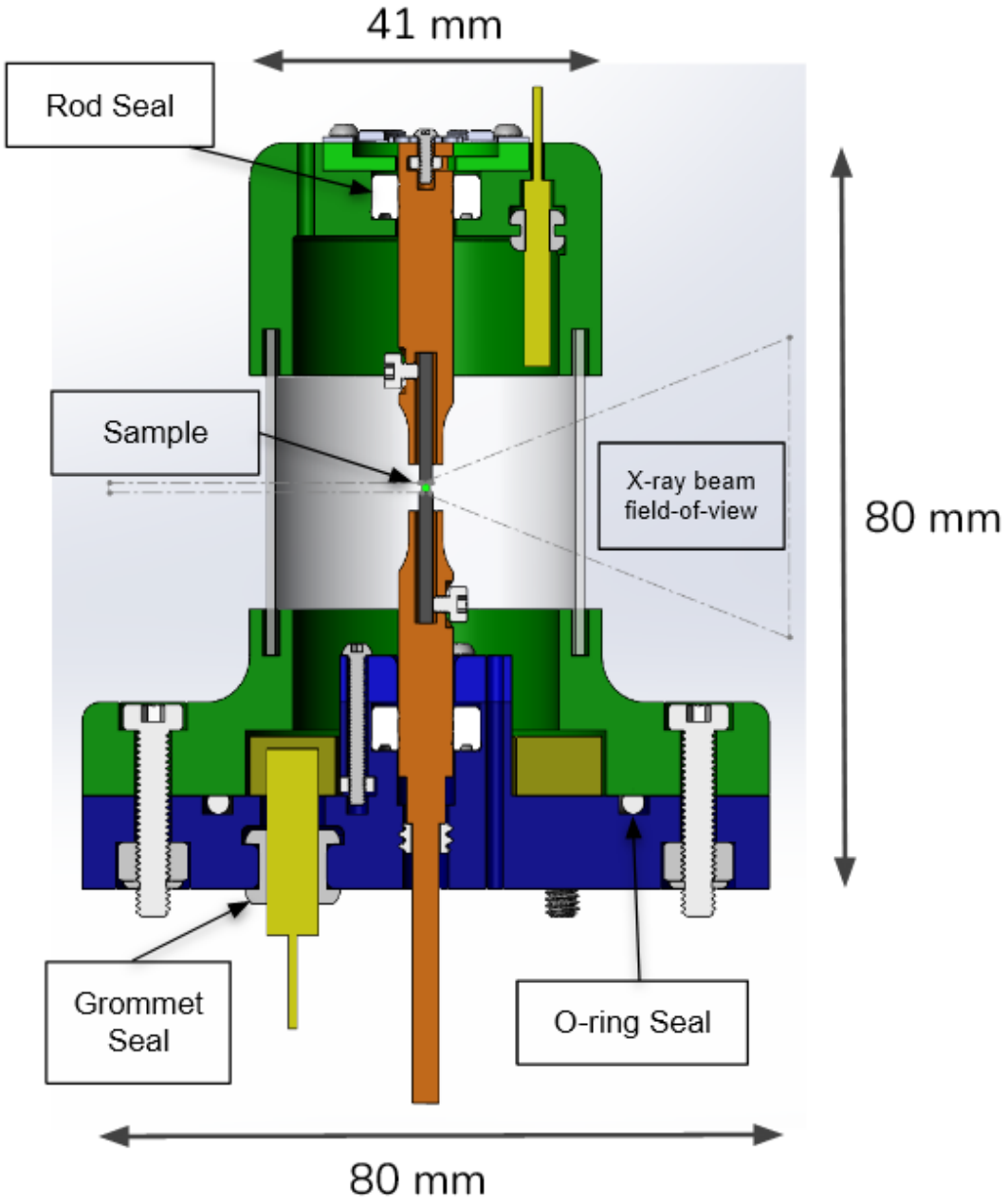

Figure 16. The sample containment subsystem features white rod seals around the orange pistons, grommets around the yellow thermistor and heat cartridge, and an o-ring in the bottom. The lid (green) is separated into two parts with the polypropylene window in-between. The container is 80mm in diameter at the bottom and 41mm in diameter at the top. The entire container is 80mm tall.

The top, transparent wall, and bottom of the container lid comprise the top shell of the sample container, with the top and bottom lid components 3D printed via stereolithography (SLA) and the transparent wall machined out of an x-ray transparent material. The container mount functions as the bottom shell of the sample container and provides accommodations for sealing to make the container interior airtight as well as mounting holes to mount the container subassembly to the actuator housing subassembly. Critical surfaces of in-house manufactured parts include contact surfaces with seals of the 3D printed parts as well as the flat faces of the polypropylene wall for alignment purposes.

The airtightness is verified as the seals are rated to block the amount of air needed, though this needs to be validated empirically. All holes and mates that do not have a seal, are going to be backfilled with silicon sealant. The x-ray transparency is verified with empirical analysis and the x-ray beam's field-of-view to ensure it does not touch any material other than the polypropylene and graphite.

Electrical application subsystem. The electrical application subsystem featured the biggest overhaul from the alpha design with the changing out of copper plates for graphite rods to ensure x-ray transparency while being electrically conductive. This required redesigning the housing to fit the rods as well as designing a method for the wires to attach to the rods. The subsystem is shown in Figure 17.

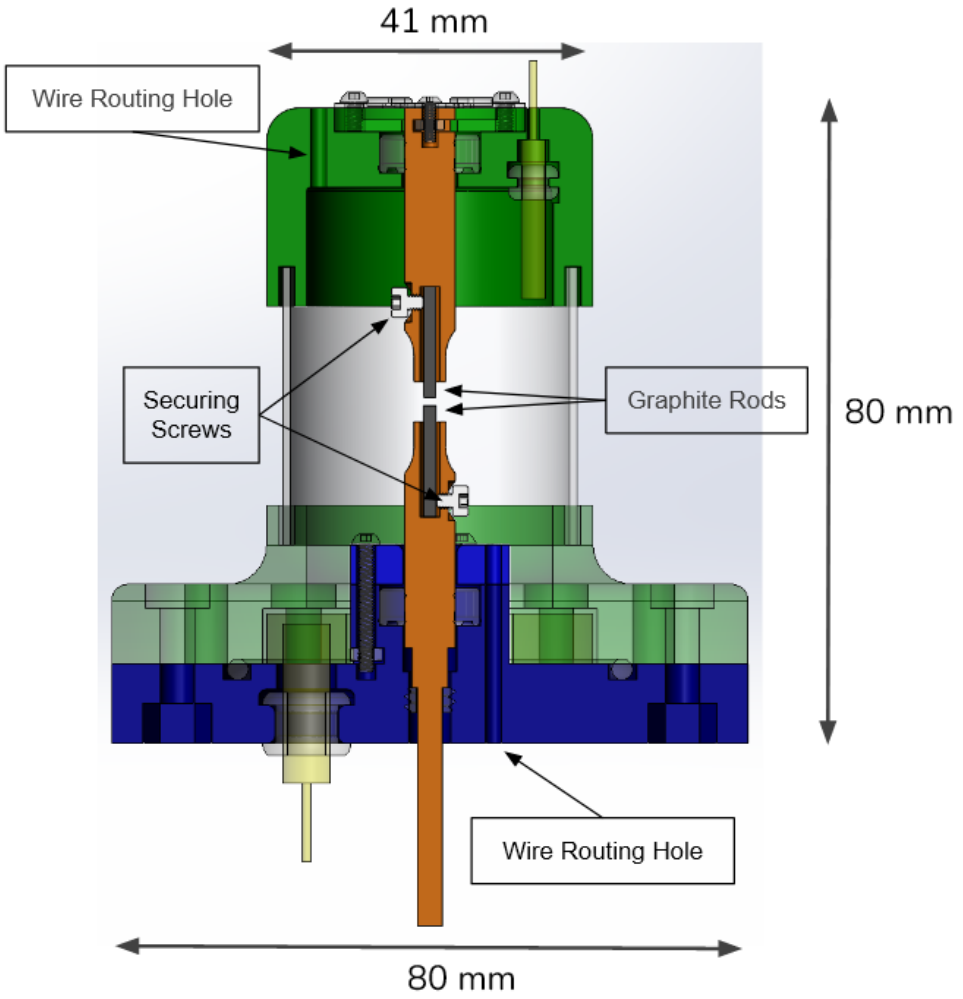

Figure 17. The electrical application subsystem with the new graphite rods to serve as the electrical contacts for the battery sample.

The anode cable attaches to the anode contact plate, routing up and out through the sample container lid to prevent the cable from interfering with the x-ray beam. Similarly, the cathode cable attaches to the cathode plate and routs down through the sample container mount. The contact rods will be machined from graphite, each bonded to its respective cable, and will touch the cell sample at its top and bottom surfaces to provide a current through the cell. The graphite rods were attached to the orange pistons using electrically conductive adhesive and the wires will be wrapped around the securing screws which will hold them in place. The wire routing holes will be backfilled with sealant to ensure the airtightness of the container.

The rods were CNC machined to length, and the fasteners were commercially purchased. Critical surfaces include the cylindrical bonding surfaces between the graphite and pistons, as well as the flat tips of the graphite rods which contact the cell sample. The physical prototype of the electrical application system enables the validation conductivity tests, to confirm that the final design is capable of running the sample with an electrical current. Moreover, construction of this subsystem, in conjunction with the sample container, enables validation of the holding requirements via testing the holding strength of a sample analogue in this subassembly.

Heat application subsystem. The heat application subsystem brings the cell sample to a steady temperature by heating a metal ring connected to a joule heating element, heating the atmosphere to a steady state temperature. The heater cartridge is inserted up through the container mount and into the solid metal heat ring located at the bottom of the sample container's interior chamber holding the cell sample. The heated air in the chamber delivers heat to the sample. The subsystem is shown in Figure 18.

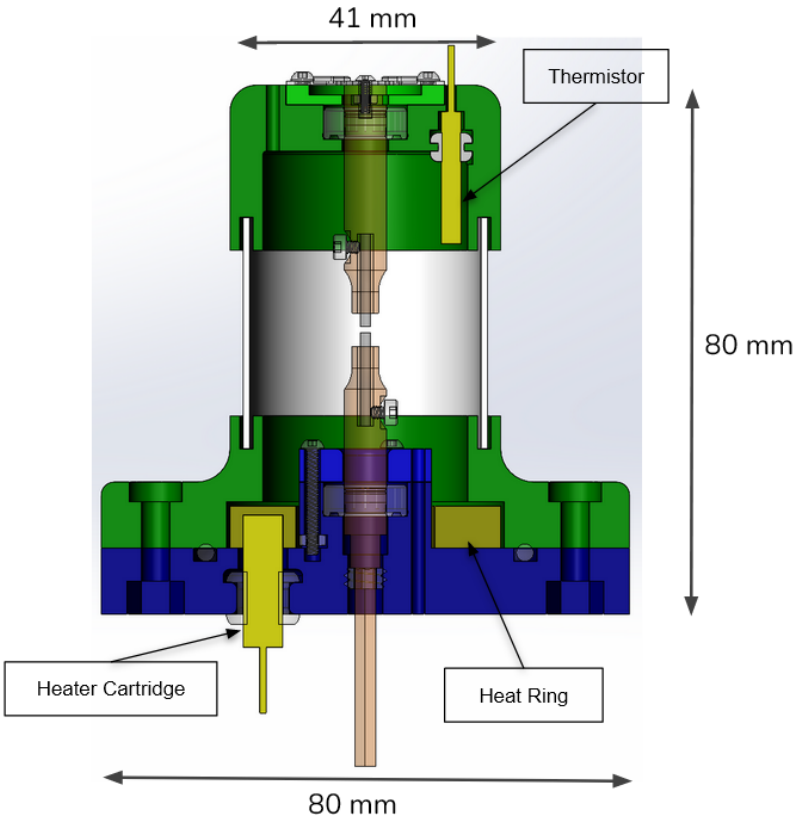

Figure 18. The heating application subsystem, consisting of a heater cartridge attached to a metal ring which heats the interior chamber of the sample container. Temperature is measured via a thermistor mounted at the top of the subsystem.

The heater cartridge and thermistor was purchased from a commercial vendor, while the heat ring was CNC machined from aluminum alloy stock. Critical surfaces include the flats of the heat ring for dimensional tolerance, and the inner surfaces of the heat ring bore to ensure flush press-fit contact with the heat cartridge. Internal chamber temperature and steady state conditions will be measured and verified by a thermistor mounted from the top through the sample container lid. This enables the physical prototype to confirm the heating requirements via empirical validation testing.

Stress Application Subsystem. The stress application subsystem uses a linear actuator to axially move the lower vertical piston, transferring force through the graphite rods and loading the sample cell with a compressive stress. A load cell is mounted to the top of the sample container lid to measure the axial load through the cell sample. This stress can be measured and controlled using the load cell.

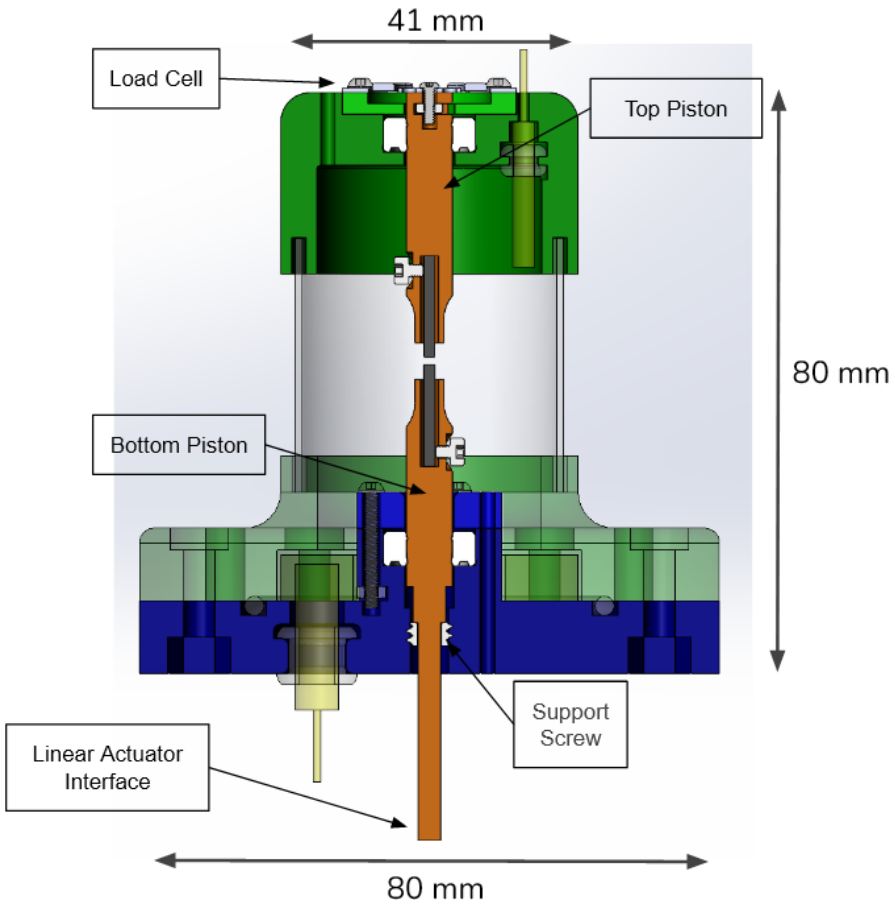

Figure 19. The stress application subsystem, which interfaces with components from the sample containment and electrical application subsystems to provide axial stress to the sample cell. Axial force is applied by the linear actuator and measured by the load cell.

The piezoelectric linear actuator motor is mounted below the container subassembly and attaches to the end effector, which penetrates through the sample container mount to transfer a vertical load to the cell sample. The piezoelectric actuator and load cell will be purchased from a commercial vendor following the empirical validation tests and approval form the sponsor. The mounting fasteners were purchased, and the pistons were SLA 3D printed. Critical surfaces include the cylindrical bonding surfaces between the graphite and pistons, as well as the flat tips of the lower and upper vertical pistons, which contact the linear actuator and load cell respectively.

The primary objective of manufacturing and assembling the stress application subsystem was to conduct preliminary empirical loading tests on the manufactured components of the final design, with manually applied force acting as substitutes for the linear actuator and load cell. The results of the empirical tests would validate the final design concepts, as well as inform the sponsor as to whether they should purchase the linear actuator and load cell for laboratory use of the x-ray microscopy device.

Verification and Validation

After manufacturing and assembling the prototype, the team designed a series of tests to verify the prototype met the requirements. When possible, they were also designed to provide values to be compared to the specification. The only requirements that were not ultimately satisfied were for keeping an airtight seal, loading the sample, and keeping the product low cost.

Hold. The samples that will be imaged using the x-ray microscope must be held precisely in place because the x-ray incident beam is 1.5mm x 0.5mm. To help verify this, the team used an analog sample made out of wire and held it between two graphite rods to test if the friction force is enough to stop the sample from sliding around. As seen in Figure 20, the analog sample was able to be held, however due to limitations in the team's manufacturing capability, the analog sample is not the same size as the actual sample. While the analog sample provides initial verification, further testing is required to ensure the actual sample will not fall out while the container is being put in place.

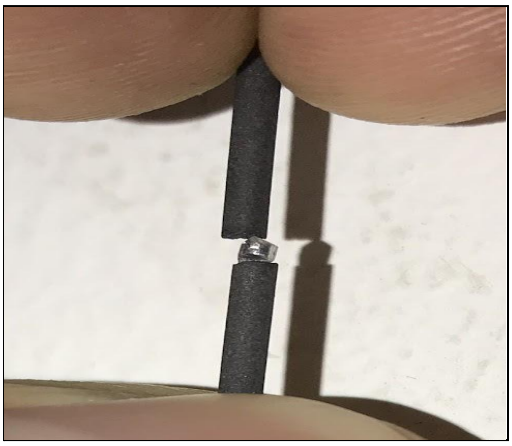

Figure 20. The analog sample (gray) made out of wire is held between two graphite rods, the lack of uniformity of the analog sample limited the precision of the results.

The sample container must also be airtight to avoid damage to the sample. To verify this, the team designed two bubble tests. For the first one, the team built the prototype container and placed it in a bucket filled with water to see if any bubbles came out. The container passed and, when opened up, everything inside of the container was dry. The second test involved placing the bucket of water (with the sample) in a vacuum chamber to induce a pressure differential and see if air escapes then. The container initially failed this test.

The sample inside of the vacuum chamber is shown in Figure 21.

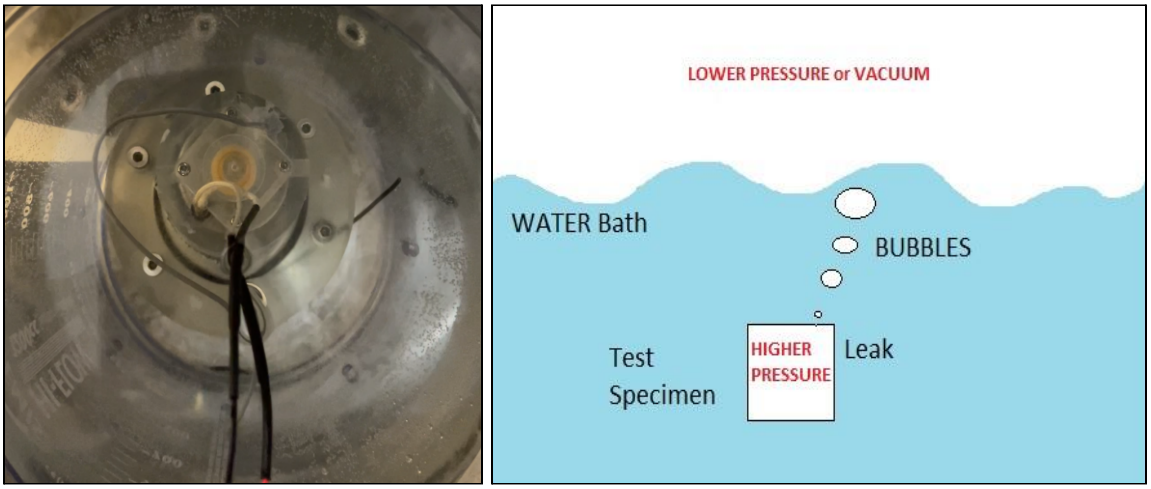

(a) (b)

Figure 21. The sample container inside of the bucket of water which is inside of a vacuum chamber shown in (a). The internals of the container, such as the graphite, are not present, only the parts that are necessary for the seal. (b) shows a schematic of the bubble test performed.

The strongest seal was the o-ring between the base and lid, the second strongest was the rod-seal around the pistons and the third strongest was the silicone seal around the window. The weakest seals were the silicone seals around the wires on the top and bottom of the container - it was these that failed. It is suggested that these holes be redesigned to specifically allow some sort of sealing epoxy to better keep in pressure. It is also suggested that a new test be devised to ensure airtightness without inducing a pressure differential to better simulate real world conditions. The device appeared to handle the initial bubble test quite well, it was only the pressure that broke the seals.

Observe. In order to be able to observe the sample, the materials that the x-ray beam passes through must be at least 90% x-ray transmissible. The main material for this is the polypropylene window which was tested in the lab by Wenxi Li, a graduate student in the Bucsek Research group. To test, he placed the window without a sample in the x-ray microscope and measured the number of photons passing through the window. This was then compared to the number of photons emitted to calculate a value of 94% transparency - above the required 90%.

The result of the x-ray transmissibility test is shown in Figure 22. It should be noted that this test was run at 24 keV, not at the specified 18 keV, however it matches the results of the team's analysis close enough that the team is confident in claiming the requirement is verified, though more testing to fully validate the specification is advised.

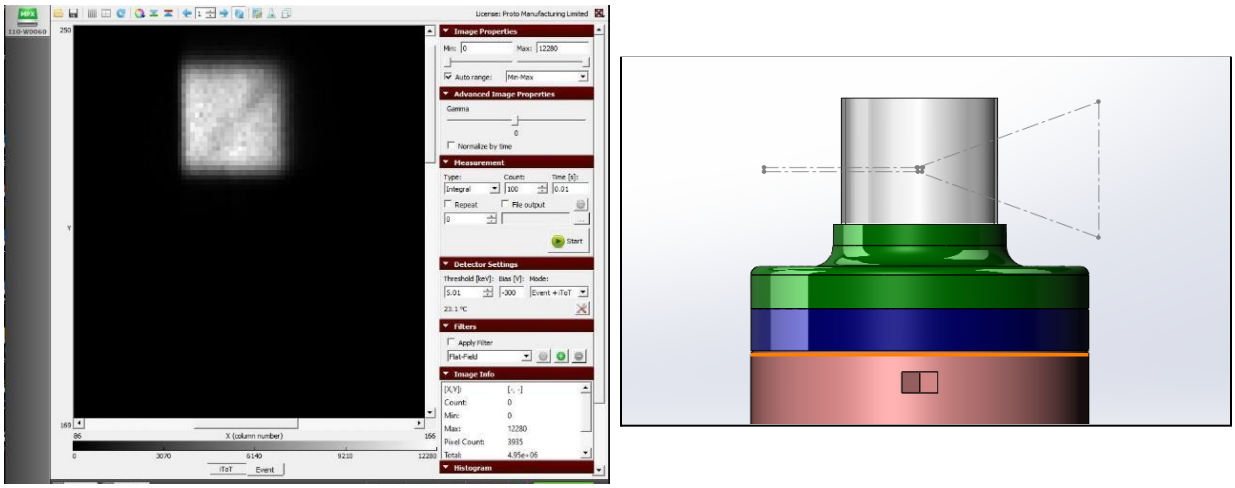

Figure 22. On the left is the console output of the transparency test. The light square surrounded by black shows the photons getting reflected by a mirror after passing through the window. On the right is a diagram of the set up with the x-ray beam outlined in gray and the polypropylene window in a clear white.

Run. Overall, the goal of the prototype device is to allow for imaging battery cell samples while they are in operando. Delivery of electrical current to the battery cell sample and for that current to travel across the anode-electrolyte-cathode layers is paramount. To verify the design's ability to run the battery cell sample, the team measured the resistance across the graphite rod. To do this the team simply used a multimeter and measured a resistance of 2.0 Ohms. As the rod that was measured was substantially longer than the graphite used in the prototype, the expected resistance of the graphite leads is expected to be much lower. Regardless, 2.0 Ohms is low enough to verify that the graphite does indeed conduct electricity. When building the prototype it is suggested to measure the resistance of the graphite when it's cut to its final length. The setup is shown in Figure 23.

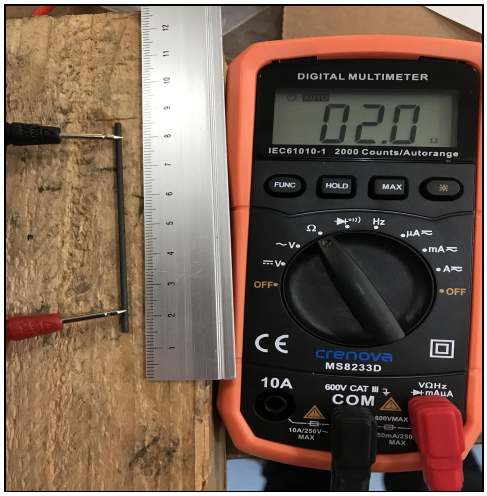

Figure 23. The setup with the graphite rod, the multimeter, and a ruler showing the length of the rod which is roughly 6 cm between the leads.

Load. The team was unable to test loading the sample, however preliminary results from assembling the device show that the load test would have almost certainly failed. This is due to the rod seal on the top piston, shown in Figure 16, providing too much friction force against the piston and it is believed that loading the sample will not actually cause the piston to move and compress the load cell. Thus the load cell will not be able to measure the force on the sample as it will not be experiencing any force itself. The team believes that this is a tolerance issue on the piston and suggests decreasing the diameter of the piston to decrease the friction. Decrease it too much, however, and the airtight seal will break. If this happens then it is suggested to forgo having the load cell on the outside of the container and move it inside, so a rod seal is unnecessary.

Heat. For heating the sample, the team tested both the heating cartridge and the thermistor to see if they can accurately increase and measure the temperature as well as have that temperature reach a steady state. This was done hooking up the thermistor to an arduino and the heating cartridge to a power supply. First the temperature of the thermistor was compared to the thermostat in the room to see if it could provide an accurate reading, which it did. Then the heating cartridge was tapped to the thermistor and voltage was supplied to the cartridge. The reading from the thermistor is shown in Figure 24, where the several steady-states are clearly shown including one above 60°C, verifying that the heating cartridge and thermistor can handle the desired temperatures. Tuning, however, will be needed to ensure it can accurately reach the temperatures in a short amount of time. It is suggested to use a PID controller to handle the temperature.

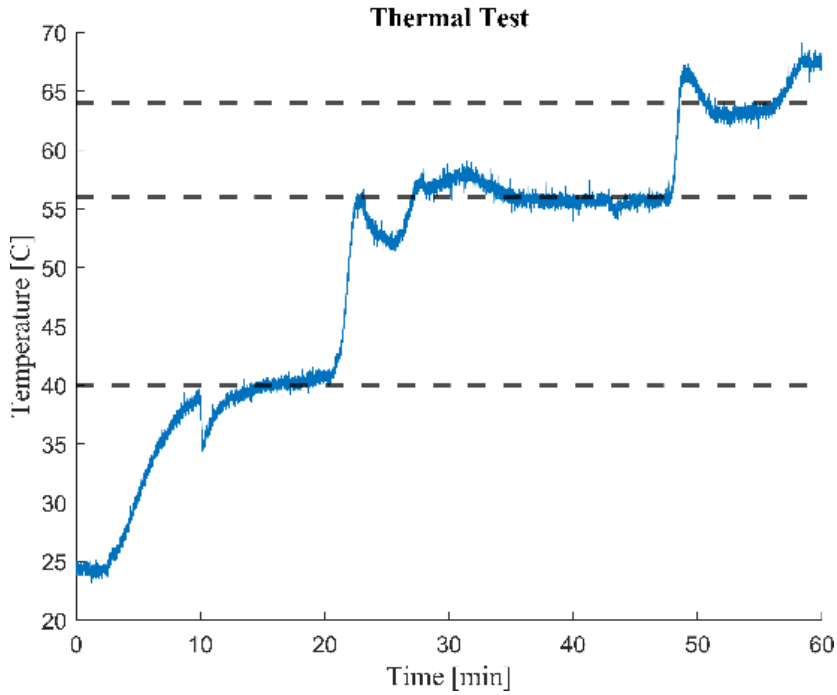

Figure 24. Temperature of the thermistor as a function of time with three clear steady-states shown at 40°C, 56°C, and 64°C. The large drops before the steady-states are mainly due to the human controller and not the heating cartridge or thermistor themselves.

Misc. requirements. The device is easy to transport at less than 10 lbs and much less than the required 35. It is also easy to assemble, however it requires 3 hex keys - one more than stated in the specification. This is not a large difference and should not affect the ease of assembly since it only requires two hex keys to assemble the container, which was the focus of the 'easy to assemble' requirement. The device failed to meet the low cost requirement as the cost of the linear actuator and load cell came to a combined

$2600 - over the specified $1000. That said, each of these are reusable and the per measurement cost will decrease drastically with each measurement. The remaining parts are well within budget at just under $137 and the total spent by the team was just under $300 - the linear actuator and load cell were not purchased, but designed for in our final prototype.

Discussion

Reinstating our problem statement: "To design and fabricate a device that holds a cell sample within the x-ray microscope, supplies a current to the cell, and applies a mechanical and thermal load during operation." We were able to successfully address all aspects of the requirements in our final design solution.

Building out the manufactured prototype for this design, we also verified and validated the design as per the requirements and specification. This is with the exception of the mechanical loading system owing to cost constraints in the proposed solution. We did accommodate for alternative solutions that would meet our budget requirements but did not want to compromise on the reliability of the loading mechanism since the specifications dealt with microns of accuracy **(**±0.05 μm**).** In the availability of more time, we would have purchased and implemented the piezoelectric motor and load cell to be tested and validated as part of the final prototype.

Preliminary empirical tests show that the polypropylene window and graphite leads will be x-ray transmissible and will not significantly interfere with photons that must pass through any tested sample cells. A water-tightness test suggests that the silicone seals, rubber grommets, and O-ring of the prototype will hold, but when placed into a pressurized environment, may fail. Further testing, with improved methodology is necessary; this may inform another iterative design change to sealant techniques. Passive heating tests demonstrate the functionality of the heating subsystem to raise the temperature of a sample containment environment to a steady-state temperature.

Our sponsor is positive about our current design solution in successfully meeting the critical functional requirements of the device. Although initially contingent, we were able to include the cell loading and heating functions into our design which were verified in the CAD model.

Possible improvements in our design include a narrower container system to increase the airtightness and packaging density of the cell. This was not considered in our final design owing to the difficulty in assembling the small-sized internal components, especially if required in a glove box for testing. The inner diameter of the container system is recommended to be the diameter of the graphite rods (1.6±0.1mm) to facilitate ease of loading the sample onto the graphite rods. Recognizing the geometric limitations imposed by a <2mm diameter container system, it is recommended that a small sleeve is added to the existing design for ease of loading the sample.

In hindsight, having known the difficulties in procuring an actual cell sample within our timeline, we would have tried to procure a sample at the very beginning of the semester to have it ready in time to test inside our device. We were still able to test the prototype with an analog cell sample of similar dimensions that successfully met our functional requirements during analysis.

Reflection

In the process of literature review, faculty interactions, design, and manufacturing, we were able to deepen our understanding of battery material technology as well as experimental methods relating to x-ray microscopy. This helped us connect our design goals and the Bucsek Research Group's focus to the broader implications of the outcomes of this project.

It is an established fact that new battery technologies are going to be a critical part of the 'decarbonization by electrification' transition in the near and distant future. Understanding the limitations of current technologies and potential of future solutions helped us educate ourselves about the energy and electronics industry.

A better battery will have a sizable impact on multiple stakeholders across multiple aspects. There are many reported cases of vehicles, devices, and energy storage systems exploding due to the limitations of current battery technology. Replacing lithium-ion batteries with more thermally stable batteries in such applications will reduce the public health and safety hazards that currently exist. Since there is a current established global standard - lithium-ion - introducing a new and improved commercially viable battery will undoubtedly experience rapid global adoption across industries. As explained in detail in the design context section, our device has minimal environmental or economic impacts across its lifecycle owing to the multiple-use application. The impacts were characterized using a stakeholder analysis map (Figure 3) and a life cycle cost analysis. The most significant resource consumption in the project was found to be the high electricity consumption required to operate the x-ray microscope during testing.

We believe that our academic, social, and cultural backgrounds within the team played an advantage throughout our design process. Having members skilled across CAD, circuits, programming, rapid prototyping, and manufacturing helped us maximize our efficiency and collaboration. With the privilege of having our sponsor's office and research laboratory on campus at the University of Michigan, we were able to maximize our communication and engagement for feedback and quick turnaround times on implementation. Our sponsor's background in Mechanical Engineering and understanding of the course expectations helped us maximize the advantage of the positive dynamics and this played a key role in the extent of design requirements we were able to address in the given project timeline. Working with team members from different countries, academic backgrounds, and standing helped create an environment that fostered learning and unique thinking styles that positively influenced our design, manufacturing, and presentation for this project. The fundamentals of strong communication, punctuality in tasks, and mutual respect and consideration for each team member's commitments helped us strike an effective balance over the course of this project. This eliminated any potential conflicts, delays, and helped us improve aspects of our individual engineering and design thinking skills in the collaborative process.

With a strong adherence to the code of ethics at the University of Michigan, College of Engineering, and of each individual, we considered all possible aspects of ethics involved in the course of our project. Establishing this prior understanding vested us with a higher sense of responsibility relating to our work in this course and on our design project.

Given the aspirational range of requirements presented at the beginning of the semester for our project, our team collectively agreed to 'never over-promise and under-deliver' to our sponsor and involved stakeholders. This helped us prevent visible short-cuts and compromise in terms of the quality of our solution and with the delivery of our final design we are convinced that we have aligned ourselves with the ethical code and considerations as engineers of the University of Michigan.

Recommendations

In terms of continuation of our delivered prototype, we recommend that the Bucsek Research Group select and procure a linear actuator that meets the mechanical loading requirements stated in the specifications (±0.05 μm displacement). Since we were unable to include this part in our assembled prototype due to time and budget constraints, we accounted for a piezo electric motor (Picomotor 8201NF) and have created a dimensioned cavity in the container to accommodate this device when purchased. Following this, a load cell (Futek FFP350) can be placed in the provided space at the top of the container system. Integrating this loading mechanism into the prototype would help our sponsor conduct verification and validation testing for this sub-system and complete all aspects of the design requirements.

To improve the accuracy of the tests conducted on our prototype, we also recommend that our sponsor load a cell sample onto the graphite leads of the device inside a glove box as initially planned, and validate the ease of assembly for the process. This is something that we did not have access to during our validation process and find it important in terms of simulating the actual experimental procedure.

Finally, following a completed validation of the prototype the device can be mounted on the rotation stage of the x-ray chamber. With a cell sample inserted into the device and electrical wiring connected to their respective terminals, the x-ray microscope can be run to investigate the diffraction pattern obtained from the cell while testing all the functional requirements of the manipulation device as a final validation.

Conclusion

The goal of this project was to design, prototype, and validate a device to hold a solid-state battery (SSB) cell sample during its real-time operation in an x-ray microscopy lab set-up that images material and chemical changes in the sample. The final design and prototype device meet the challenges of imaging battery cell samples in real time while they are being used - providing critical new information that allows researchers to better understand the changes in the battery material properties and specifically the interface layer between anode/cathode and electrolyte. Analyzing the behavior of battery materials during operation presents opportunities for better material selection, resulting in improvements of many battery performance metrics including energy density, cycle life, stability, and safety.

The primary design requirements from the Bucsek research group include: (i) hold SSB sample cells of varying geometries; (ii) supply current to the sample cell under test; (iii) be transparent to the x-ray radiation in order to avoid interference with incident or diffracted x-rays; and, (iv) prevent the battery cell sample from interacting with oxygen gas. Additionally, the device should be capable of applying a mechanical load to the SSB sample cell as well as apply heat to the sample. Other requirements include a design and prototype that is low cost, easy to assemble, and easily transported.

After thorough design concept ideation including a divergent thinking process, elimination of unworkable designs, and a narrowing of design concepts through evaluation matrices, an alpha design was selected and a basic virtual model was produced with CAD. The alpha design was decomposed into five functional requirements based on the overarching requirements and specifications: holding the sample, observing the sample, electrically running the sample, mechanically loading the sample, and heating the sample. Engineering analysis of the alpha design was performed to assess its ability to adequately perform these five subfunctions. This analysis informed iterative design choices that improved upon the alpha design.

A final virtual design model was developed and again represented with CAD. From the CAD, a bill of materials and manufacturing plans were developed, and an eventual prototype was assembled. The

prototype device and the virtual design are both delivered to the Bucsek Research Group for their continued use and evaluation.

We believe that we have successfully worked together as a team to deliver a working prototype of a device that can accomplish in-situ and operando studies of battery cell samples in the Bucsek Research Group's X-ray Microscopy Lab setup. The resultant prototype design fulfills the critical requirements that were laid out in the beginning of the semester. A virtual solution for the mechanical loading system was proposed since it could not be assembled physically under budget. Future work can help determine the stress limits of sample cells and the accuracy of proposed linear actuators. The prototype device was also delivered to the Bucsek Research Group on time and under budget.

Acknowledgements

We are thankful to the Bucsek Research Group (Prof. Ashley Bucsek, Wenxi Li) for the opportunity to work on this project as a part of our course, along with their constant support in our design process. We would also like to thank our ME 450 section instructor Prof. K. Alex Shorter for his continued guidance and feedback on our approach to all aspects of this project and leading up to the completion of this report. We also thank the ME 450 course coordinators - Prof. Skerlos, Prof. Sienko, Graduate Student Instructors Jeremy and Nick, and Librarian Joanna Thielen for the guiding content towards our approach in engineering projects. We are grateful to the Department of Mechanical Engineering at the university for the opportunity to engage in this enriching course alongside the distinguished faculty.

References

1. Matthews, Ian. 2020. "In Simple Terms: Everything You Need To Know About Solid State EV Batteries". *Partisan Issues*. https://www.partisanissues.com/2020/10/in-simple-terms-everything-you-need-to-know-about-solid-state-ev-batteries/
2. Challa, V., 2022. How to Select the Right Battery for Your Application? Part 1: Important Battery Metric Considerations. [online] Dfrsolutions.com. Available at: <https://www.dfrsolutions.com/blog/how-to-select-the-right-battery-for-your-application-part-1-battery-metric-considerations> [Accessed 5 February 2022].
3. Challa, V., 2022. *How to Select the Right Battery for Your Application? Part 1: Important Battery Metric Considerations*. [online] Dfrsolutions.com. Available at: <https://www.dfrsolutions.com/blog/how-to-select-the-right-battery-for-your-application-part-1-battery-metric-considerations> [Accessed 5 February 2022].
4. Araujo, Keith. “Battery Cell Comparison.” Epec Engineered Technologies. Epec, LLC. Accessed February 1, 2022. https://www.epectec.com/batteries/cell-comparison.html.
5. “Laptops for Consumers - Long Battery Life Icon.” ClipartMax.com. ClipartMax. Accessed February 5, 2022. https://www.clipartmax.com/middle/m2i8H7i8H7m2i8A0_laptops-for-consumers-long-battery-life-icon/.
6. “Li Ion Recycle Symbol Clipart (#796921) - Pikpng.” PikPng.com. PikPng. Accessed February 1, 2022. https://www.pikpng.com/pngvi/bJRmJx_li-ion-recycle-symbol-clipart/.
7. O'shea, Paul. “Pushing to the Very Edge of Safe Li-Ion Charging.” Power Electronics News. AspenCore, January 19, 2018. https://www.powerelectronicsnews.com/pushing-to-the-very-edge-of-safe-li-ion-charging/.
8. "Infographic: High Demand For Lithium-Ion Batteries". 2020. *Statista Infographics*. https://www.statista.com/chart/23808/lithium-ion-battery-demand/.
9. Liu, Jia, Hong Yuan, He Liu, Chen‐Zi Zhao, Yang Lu, Xin‐Bing Cheng, Jia‐Qi Huang, and Qiang Zhang. 2021. "Unlocking The Failure Mechanism Of Solid State Lithium Metal Batteries". *Advanced Energy Materials* 12 (4): 2100748. doi:10.1002/aenm.202100748.
10. Pender, Joshua P., Gaurav Jha, Duck Hyun Youn, Joshua M. Ziegler, Ilektra Andoni, Eric J. Choi, and Adam Heller et al. 2020. "Electrode Degradation In Lithium-Ion Batteries". ACS Nano 14 (2): 1243-1295. doi:10.1021/acsnano.9b04365.
11. Shapovalov, Viktor, Kristina Kutukova, Sebastian Maletti, Christian Heubner, Vera Butova, Igor Shukaev, Alexander Guda, Alexander Soldatov, and Ehrenfried Zschech. 2021. "Laboratory X-Ray Microscopy Study Of Microcrack Evolution In A Novel Sodium Iron Titanate-Based Cathode Material For Li-Ion Batteries". Crystals 12 (1): 3. doi:10.3390/cryst12010003.
12. Bucsek, Ashley.. "ME 450 Battery Performance Project". Email, 2022.
13. Dixit, Marm, Bairav Vishugopi, Peter Kenesei, Jun-Sang Park, Jonathan Almer, Partha Mukherjee, and Kelsey Hatzell. 2021. "Supporting Information: Polymorphism Of Garnet Solid Electrolytes And Its Implications On Grain Level Chemo-Mechanics". U.S. Department of Energy. https://chemrxiv.org/engage/chemrxiv/article-details/617586480c0480187a42ef5a.
14. Lewis, John A., Francisco Javier Quintero Cortes, Yuhgene Liu, John C. Miers, Ankit Verma, Bairav S. Vishnugopi, and Jared Tippens et al. 2021. "Linking Void And Interphase Evolution To Electrochemistry In Solid-State Batteries Using Operando X-Ray Tomography". Nature Materials 20 (4): 503-510. doi:10.1038/s41563-020-00903-2.
15. Oberhaus, D., 2020. Did QuantumScape Just Solve a 40-Year-Old Battery Problem?. [online] Wired. Available at: <https://www.wired.com/story/quantumscape-solid-state-battery/> [Accessed 6 February 2022].
16. L.P., P., 2022. Piezo Motors | Linear Motor Positioners | Manufacturer. [online] Pi-usa.us. Available at: <https://www.pi-usa.us/en/products/piezo-motors-stages-actuators/> [Accessed 8 February 2022].
17. TDI International, Inc. 2022. TDI Glove Boxes - Why Choose TDI for Your Lab/Mailroom Glove Box?. [online] Available at: <https://www.tdiinternational.com/gloveboxes/choose-tdi-glove-boxes/> [Accessed 7 February 2022].
18. EI Sensor Technologies. 2022. Thermistor Probes - Temperature Probe Assemblies | EI Sensor Technologies. [online] Available at: <https://www.ei-sensor.com/thermistor-probes/> [Accessed 6 February 2022].
19. Cooper, Heather, Shanna Daly, Steven Skerlos, and Kathleen Sienko. 2020. "ME Capstone Design Process Framework". Presentation, University of Michigan North Campus, 2020.
20. Wynn D., Clarkson J. (2005) Models of designing. In: Clarkson J., Eckert C. (eds) Design process improvement. Springer, London. https://doi-org.proxy.lib.umich.edu/10.1007/978-1-84628-061-0_2
21. “Bubble Leak Testing using an acrylic vacuum chamber,” Bubble leak testing using an acrylic vacuum chamber, 01-Mar-2018. [Online]. Available: https://www.sanatron.com/articles/bubble-leak-testing-using-an-acrylic-vacuum-chamber.php. [Accessed: 05-Apr-2022].
22. Henke.lbl.gov. 2022. CXRO X-Ray Interactions With Matter. [online] Available at: <https://henke.lbl.gov/optical_constants/> [Accessed 5 April 2022].

Appendix A

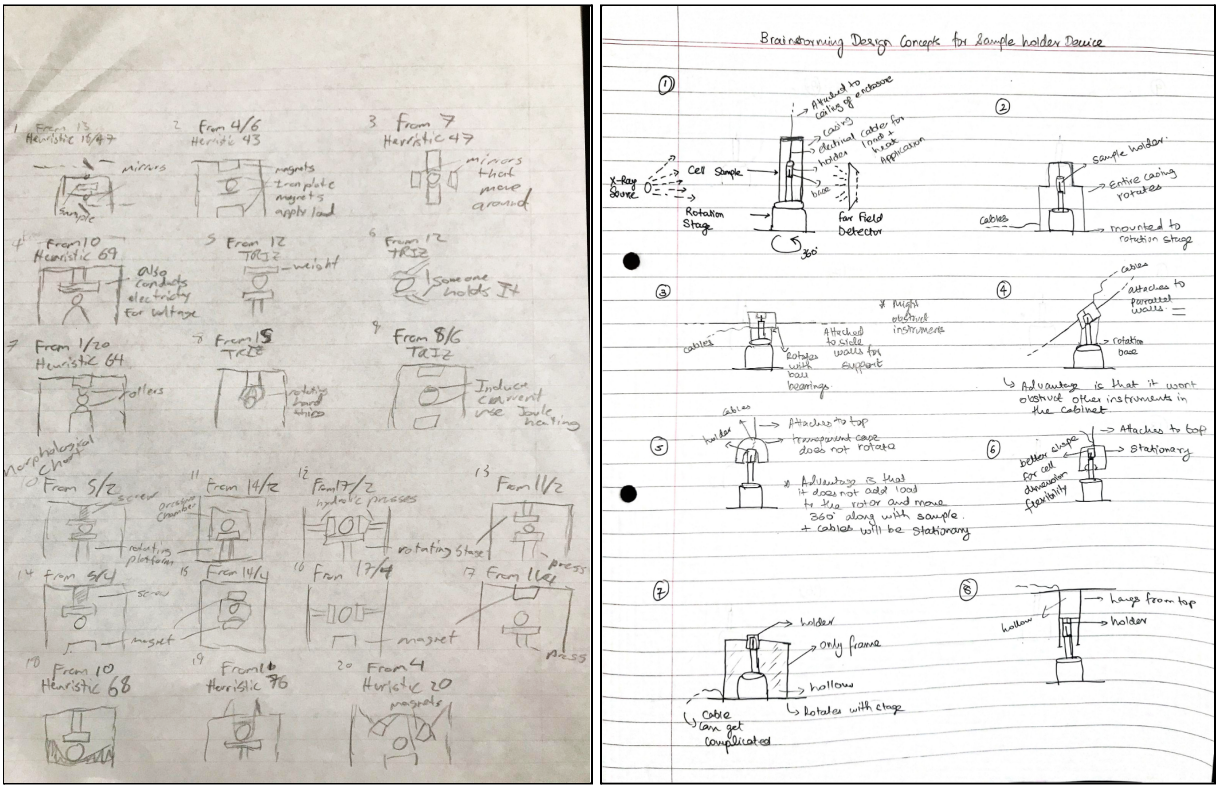

Figure A1. Basic designs developed with divergent thinking.

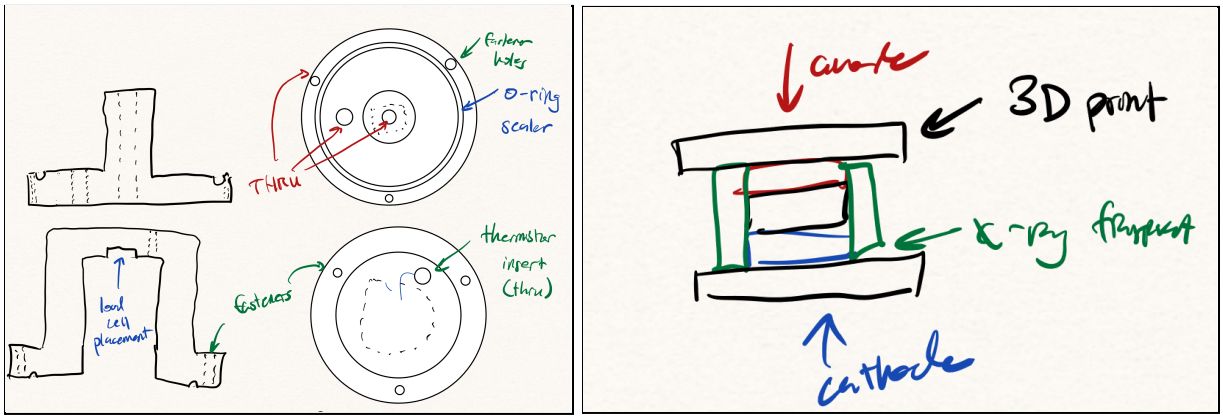

Figure A2. Two designs for the "holding the sample" sub-function. The left design has a thicker wall surrounding the sample then the others to give greater stability and the fewer parts make it easier to manufacture and assemble. It does, however, suffer from decreased x-ray transparency due to the thicker walls. The right design is significantly smaller than the others in order to provide stability while decreasing the overall wall thickness. It suffers from difficulty of assembly and difficulty of applying heat to the sample.

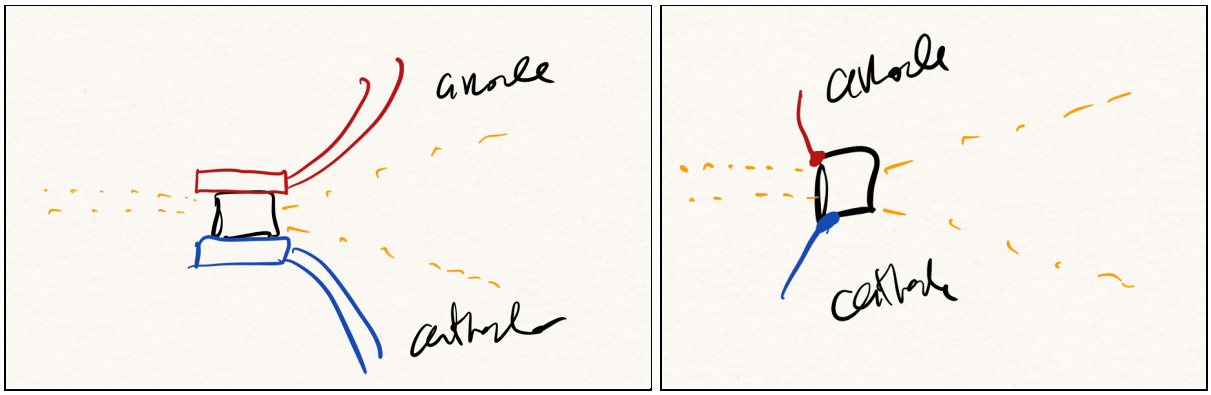

Figure A3. Two designs for the "running the sample" sub-function. The left design has thick plates with the sample sandwiched between them. This provides greater stability to support the sample, but runs the risk of having the leads interfere with the x-ray beam as the material they are made of is x-ray transparent. The right design tries to fix this by only having a single contact point for the leads near where the beam initially hits the sample. However, this causes issues with supporting the sample and handling the rotation of the sample as the leads would have to rotate as well.

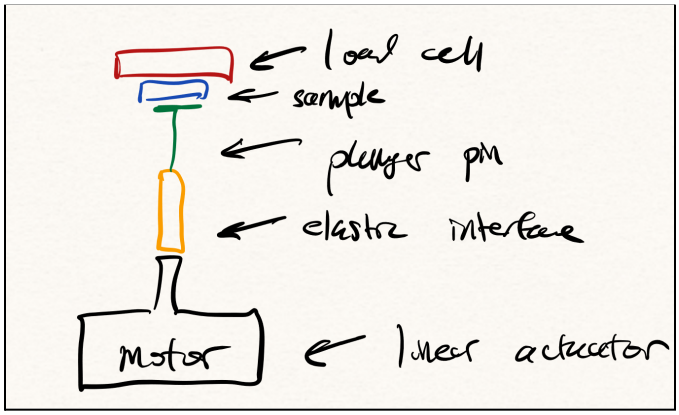

Figure A4. A second design for the "loading the sample" sub-function. This design features an elastic interface between the linear actuator and the plunger pin. This is done in order to decrease the precision needed for the actuator to obtain the loads required. However, accuracy remains an issue as well as repeatability as the material fatigues. The load cell on top should be able to help though.

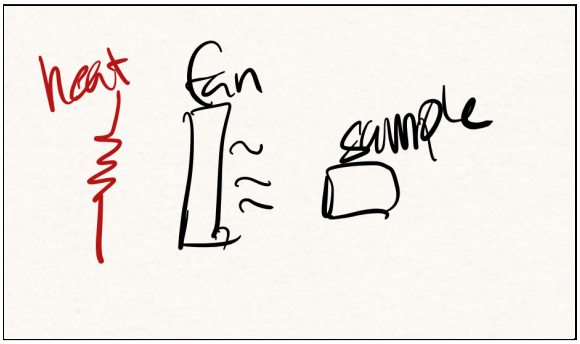

Figure A5. A second design for the "heating the sample" sub-function. This design features a fan blowing hot air onto the sample. This will decrease the amount of heat the heating element needs to put out compared to other designs, but accuracy and consistency of the heat are an issue.

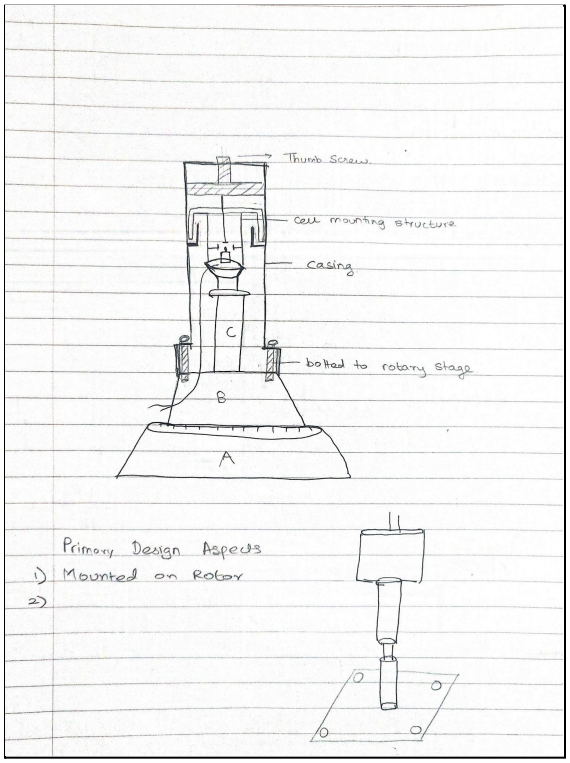

Figure A6. Hand drawn alpha concept of x-ray microscopy device. The main purpose of this process is to integrate the four selected functional concepts into a single package and confirm that the design of the entire system still meets the sponsor requirements and engineering specifications.

Table A1. The evaluation matrix for the "running the sample" sub-function. Design 1 refers to the design shown on the top right of Figure 5. Design 2 refers to the design shown on the right of Figure A3. Design 3 refers to the figure on the left of Figure A3.

Criteria	**Design 1**	Design 2	Design 3
Ease of manufacturing (0.1)	2	5	4
Support of sample (0.4)	4	1	5
x-ray transparency (0.5)	3	4	1
Weighted Total	3.2	2.9	2.9
Rank	**1**	2	2

Table A2. The evaluation matrix for the "loading the sample" sub-function. Design 1 refers to the design shown on the bottom left of Figure 5. Design 2 refers to the design shown in Figure A4.

Criteria	**Design 1**	Design 2
Ease of manufacturing (0.1)	5	3
Accuracy of applied force (0.5)	5	2
Repeatability (0.2)	5	3
Cost (0.2)	1	4
Weighted Total	4.2	2.7
Rank	**1**	2

Table A3. The evaluation matrix for the "heating the sample" sub-function. Design 1 refers to the design shown on the bottom right of Figure 5. Design 2 refers to the design shown in Figure A5.

Criteria	**Design 1**	Design 2
Ease of manufacturing (0.1)	3	4
Heat distribution (0.5)	4	4
Accuracy of temperature (0.4)	4	3
Weighted Total	3.9	3.6
Rank	**1**	2

Appendix B

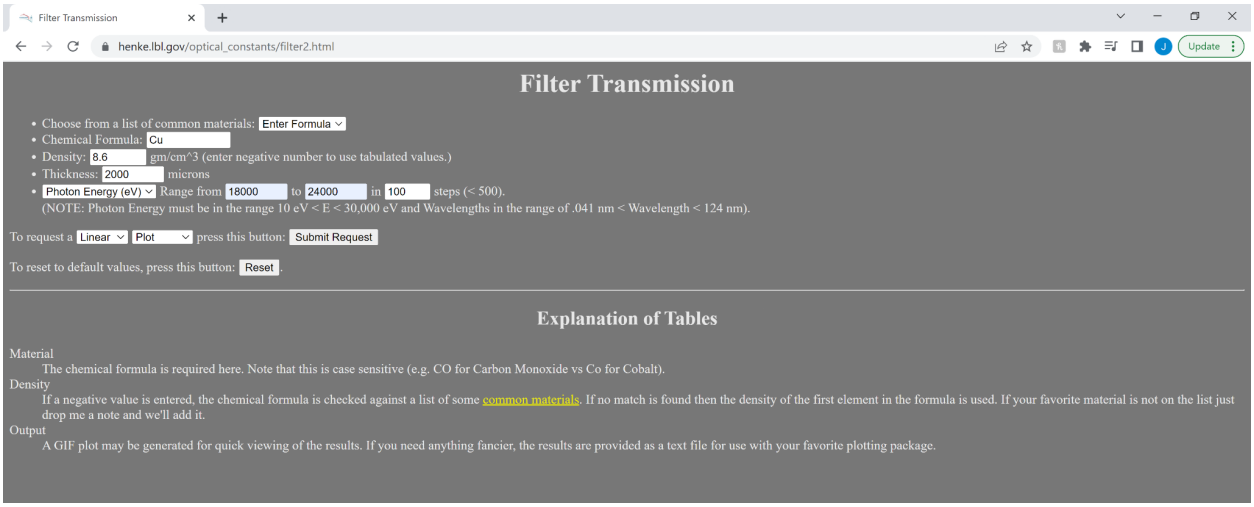

Figure B1. The Berkeley Lab's CRXO X-ray Transmission of a solid material calculator. This shows the calculation for pure copper, the metal selected for the contact plates in the alpha design. The inputs are: the chemical formula *Cu*, the density 8.6 gm/cm^3, and the estimated thickness of 2000 microns.

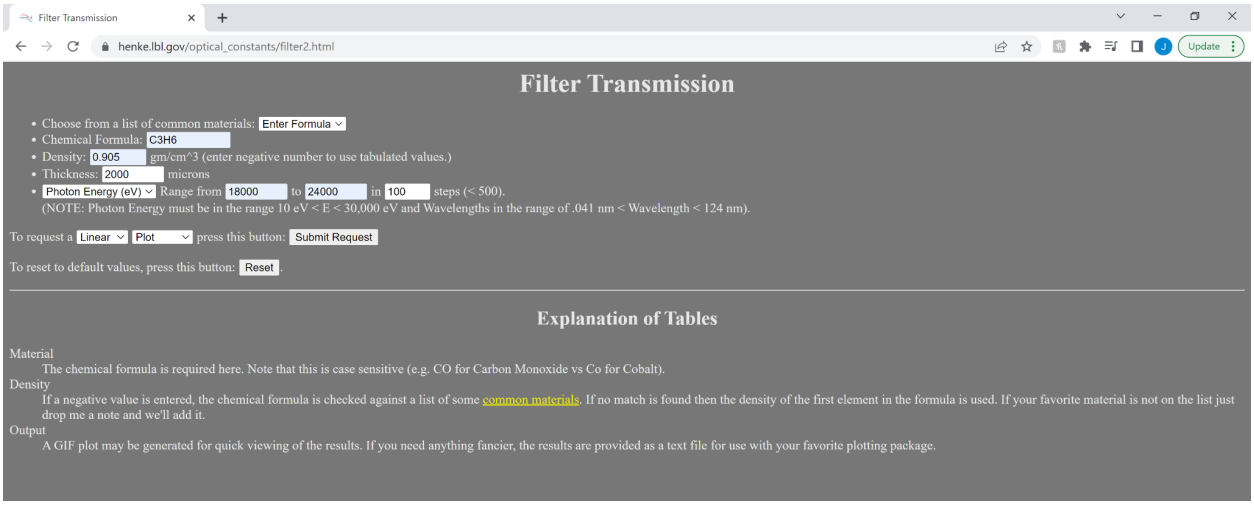

Figure B2. The Berkeley Lab's CRXO X-ray Transmission of a solid material calculator. This shows the calculation for polypropylene, the material selected for the 360-degree transparent window that would encompass the sample containment device. The inputs are: the chemical formula C_3H_6, the density 0.905 gm/cm^3, and the estimated thickness of 2000 microns.

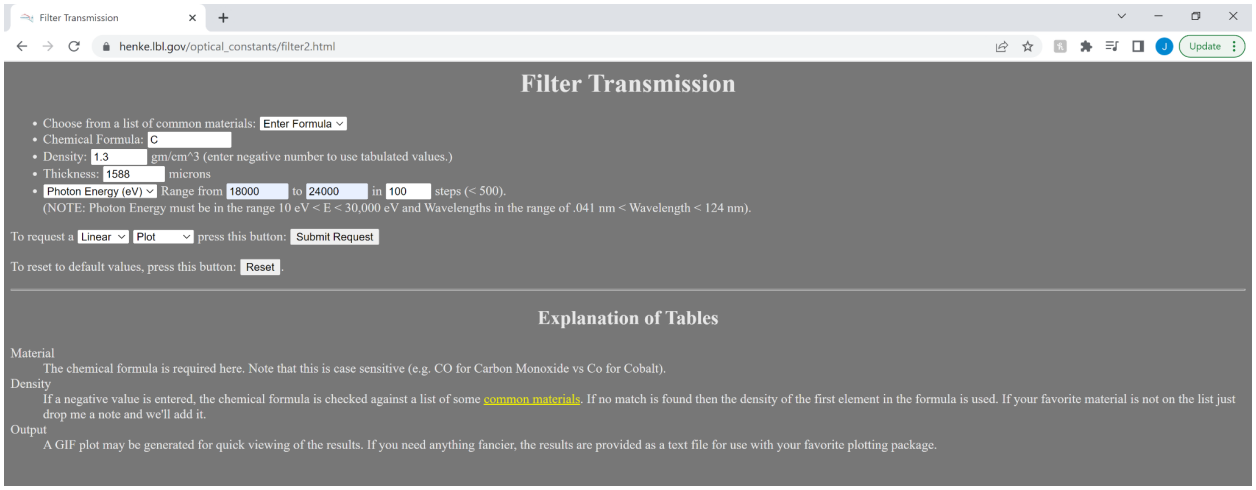

Figure B2. The Berkeley Lab's CRXO X-ray Transmission of a solid material calculator. This shows the calculation for graphite, the alternative material investigated for supplying electrical current to the sample. The inputs are: the chemical formula *C*, the density 1.3 gm/cm^3, and the estimated thickness of 1588 microns.

Appendix C

Table C1. ME 450 Team 18 Plastics and Polypropylene Order through Mechanical Engineering Online Purchasing System. Order submitted and approved by ME administrators on 03/017/22.

Line #	Qty.	Unit	Item #	Item Descr.	URL	Price/Unit	Total
1	1	FT	8658K57	Polypropylene Rod 1-1/2" Diameter	Link	$11.89	$11.89
2	10	FT	5392K59	Hard Polypropylene Plastic Tubing for Air&Water	Link	$1.65	$16.50
Shipping							$0.00
Total Cost							$28.39

Table C2. ME 450 Team 18 Prototype Assembly Materials Order through Mechanical Engineering Online Purchasing System. Order submitted and approved by ME administrators on 04/08/22.

Line #	Qty.	Unit	Item #	Item Descr.	URL	Price/Unit	Total
1	1	PKG	91301A029	Hollow-Lock Set Screw, Black-Oxide Alloy Steel, 1/4"-20 Thread, 1/8" Long	Link	$10.00	$10.00
2	2	PKG	1995N31	Polyurethane Rod Seal for 1/4" Rod Diameter, 0.250" ID x 0.500" OD x 0.188" Wide	Link	$6.89	$13.78
3	1	PKG	9600K73	SBR Rubber Grommet for 5/32" Hole Diameter and 3/64" Material Thickness	Link	$18.21	$18.21
4	1	PKG	9307K866	Buna-N Rubber Grommets for 5/16" Hole Diameter and 3/16" Material Thickness, 3/16" ID	Link	$1.33	$1.33
5	1	PKG	9452K138	Oil-Resistant Buna-N O-Ring, 3/32 Fractional Width, Dash Number 133	Link	$13.38	$13.38
6	1	EA	9121K99	Conductive Graphite, 1/16" Diameter Rod, 6" Long	Link	$19.27	$19.27
7	1	PKG	92095A454	Button Head Hex Drive Screw, Passivated 18-8 Stainless Steel, M2 x 0.40 mm Thread, 8mm Long	Link	$6.38	$6.38
8	1	PKG	92095A111	Button Head Hex Drive Screw, 18-8 Stainless Steel, M2 x 0.4 Thread Size, 16mm Long	Link	$4.28	$4.28
9	1	PKG	92095A323	Button Head Hex Drive Screw, Passivated 18-8 Stainless Steel, M1.6 x 0.35 mm Thread, 5mm Long	Link	$11.12	$11.12
10	1	PKG	91828A111	18-8 Stainless Steel Hex Nut, M2 x 0.4 mm Thread	Link	$6.14	$6.14
11	1	PKG	91828A006	18-8 Stainless Steel Hex Nut, M1.6 x 0.35 mm Thread	Link	$14.86	$14.86

12	**1**	**PKG**	**92855A419**	**18-8 Stainless Steel Low-Profile Socket Head Screws with Hex Drive, M4 x 0.7 mm Thread, 20 mm Long**	**Link**	**$5.07**	**$5.07**
13	**1**	**PKG**	**90576A103**	**Medium-Strength Steel Nylon-Insert Locknut, Class 8, Zinc Plated, M4 x 0.7 mm Thread, 5 mm High**	**Link**	**$5.57**	**$5.57**
14	**1**	**PKG**	**92290A848**	**Super-Corrosion-Resistant 316 Stainless Steel Socket Head Screw, M2 x 0.40 mm Thread, 2 mm Long**	**Link**	**$7.55**	**$7.55**
15	**1**	**PKG**	**7829K1**	**Twist-on No-Crimp Butt Splices for 24-18 Wire Gauge**	**Link**	**$10.22**	**$10.22**
16	**1**	**EA**	**8251T1**	**Red, 25ft Solid Wire, 300V AC, 24 Wire Gauge**	**Link**	**$2.57**	**$2.57**
17	**1**	**EA**	**8251T1**	**Black, 25ft Solid Wire, 300V AC, 24 Wire Gauge**	**Link**	**$2.57**	**$2.57**
18	**1**	**EA**	**7661A13**	**Conductive Adhesive for Electronics, 0.09 oz.. One-Time-Use Packet**	**Link**	**$41.61**	**$41.61**
Shipping							**$0.00**
Total Cost							**$193.91**

Bill of Materials

Table 3. Bill of Materials for the prototype device. Parts numbered 1 through 17 are major parts of the prototype device. These include parts that were made from purchased stock materials and then manufactured, parts that were 3D printed, or commercial electronics. Parts with specific alpha-numeric part identifiers were purchased through a vendor. The price per unit and total price of the number of that specific component are included in the two rightmost columns. Total number of components and the price of the prototype are included at the bottom.

Part No.	Part Title	Material	Supplier	Quantity	Unit Price	Price
1	X-ray transparent window	Polypropylene	McMaster-Carr	1	$11.89	$11.89
2	Conductive graphite rods	Graphite	McMaster-Carr	2	$4.82	$9.64
7661A13	Conductive epoxy adhesive	Epoxy	McMaster-Carr	1	$41.61	$41.61
92290A848	Corrosion Resistant Socket Head Screw	Stainless Steel	McMaster-Carr	2	$0.30	$0.60
8251T1	24-gauge black wire	Solid wire	McMaster-Carr	1 foot	$0.51	$0.51
8251T1	24-gauge red wire	Solid wire	McMaster-Carr	1 foot	$0.51	$0.51
3	Top piston	SLA Resin	Self-supplied	1	$1.00	$1.00
4	Bottom piston	SLA Resin	Self-supplied	1	$1.00	$1.00
1995N31	Rod seal	Polyurethane	McMaster-Carr	2	$3.45	$6.89
91301A029	Hollow-lock set screw	Black-Oxide Alloy Steel	McMaster-Carr	1	$0.40	$0.40
5	Top Rod seal cover	SLA Resin	Self-supplied	1	$0.50	$0.50
6	Bottom Rod seal cover	SLA Resin	Self-supplied	1	$0.50	$0.50
7	Metal heating ring	Aluminum	ME Undergraduate Machine Shop	1	$0.59	$0.59
8	Heating cartridge	Commercial Electronic	Self-supplied	1	$3.00	$3.00
9	Thermistor	Commercial Electronic	Self-supplied	1	$13.00	$13.00
10	Container lid top	SLA Resin	Self-supplied	1	$1.50	$1.50
9600K73	SBR Rubber Grommets	SBR Rubber	McMaster-Carr	1	$0.36	$0.36
92095A454	M2, 8mm Button Head Hex Screw	Stainless Steel	McMaster-Carr	4	$0.26	$1.04
92095A323	M1.6, 5mm Button Head Hex Screw	Stainless Steel	McMaster-Carr	1	$0.22	$0.22

91828A006	M1.6 Hex Nut	Stainless Steel	McMaster-Carr	1	$0.59	$0.59
11	Container lid bottom	SLA Resin	Self-supplied	1	$2.00	$2.00
12	Container base	SLA Resin	Self-supplied	1	$2.00	$2.00
9452K138	Oil-Resistant Buna-N O-Ring	Buna-N Rubber	McMaster-Carr	1	$0.13	$0.13
9307K866	Buna-N Rubber Grommets	Buna-N Rubber	McMaster-Carr	1	$0.13	$0.13
92095A111	M2, 16mm Button Head Hex Screw	Stainless Steel	McMaster-Carr	3	$0.04	$0.12
91828A111	M2 Hex Nuts	Stainless Steel	McMaster-Carr	7	$0.06	$0.42
92855A419	M4, 20mm Socket Head Screws	Stainless Steel	McMaster-Carr	6	$0.20	$1.20
13	Actuator mount	PLA	Self-supplied	1	$0.97	$0.97
14	Actuator collar	PLA	Self-supplied	1	$0.03	$0.03
91292A130	M4, 30mm Socket Head Screws	Stainless Steel	McMaster-Carr	4	$0.14	$0.55
90576A103	M4 Insert Locknut	Zinc-plated Steel	McMaster-Carr	10	$0.04	$0.36
15	Front actuator shell	PLA	Self-supplied	1	$5.05	$5.05
16	Rear actuator shell	PLA	Self-supplied	1	$5.23	$5.23
91292A020	M3, 25mm Socket Head Screws	Stainless Steel	McMaster-Carr	2	$0.09	$0.18
91292A192	M5, 30mm Socket Head Screws	Stainless Steel	McMaster-Carr	9	$0.22	$1.95
91828A241	M5 Nuts	Stainless Steel	McMaster-Carr	9	$0.09	$0.82
17	Rotation mount	PLA	Self-supplied	1	$18.63	$18.63
91292A128	M5, 20mm Socket Head Screws	Stainless Steel	McMaster-Carr	6	$0.17	$1.00
			Total Quantity:	**89**	**Total Cost:**	**$136.12**

Manufacturing Plan

Machined Parts

- Polypropylene Window - Lathe (CNC optional)
    - Start with a 1 ½” or larger polypropylene rod
    - Face off one side
    - Bring outer diameter to size
    - Drill a center hole large enough for a boring bar
    - Turn the inner diameter up to size
    - Part to the correct length
- Heat Ring - Mill (CNC optional)
    - Start with ¼” aluminum sheet
    - Waterjet ring geometry
    - Mount ring in with V-blocks in mill vise
    - CNC the blind bore, or drill and ream
- Graphite Rods - Mill
    - Cut 1/16” graphite rod oversized
    - Mount graphite rod with small (or custom) V-blocks in mill vise
    - Mill a flat on to the end of the rod
    - Rotate rod and mill a flat on the other end of the rod

SLA Printed Parts

- Container Lid Top
- Container Lid Bottom
- Container Base - Note the center hole in the bottom must be tapped with a ¼”-20 tap
- Top Piston
- Bottom Piston
- Top Rod Seal Cover
- Bottom Rod Seal Cover

FDM Printed Parts

- Rotation Mount
- Actuator Mount
- Actuator Coller
- Front Actuator Shell
- Rear Actuator Shell